FORCE ACTIVATION OF I DOMAIN CONTAINING AND LACKING INTEGRINS ON LIVE CELLS

A Thesis
Presented to
The Academic Faculty

by

William Parks

In Partial Fulfillment
of the Requirements for the Degree
Masters in Mechanical Engineering in the
George W. Woodruff School of Mechanical Engineering

Georgia Institute of Technology
December 2010

Force Activation of I-Domain Containing and Lacking Integrin on Live Cells

Approved by:

Dr. Cheng Zhu, Advisor
School of Mechanical Engineering
Georgia Institute of Technology

Dr. Jennifer Curtis
School of Physics
Georgia Institute of Technology

Dr. Todd Sulchek
School of Mechanical Engineering
Georgia Institute of Technology

Date Approved: July 7, 2010

To the students of the Georgia Institute of Technology, my lab mates and, most importantly, my family.

ACKNOWLEDGEMENTS

I would like to thank Dr. Zhu for giving me the opportunity to do this. He has shown incredible kindness and patience through the course of this work and has taught me an incredible amount. I would like to thank both my old friends from Alabama as well as the friends I have made while at the Georgia Institute of Technology. They have helped me more then they will ever realize. I'd also like to thank my family for the immeasurable support and understanding they have given me. Were it not for my family and their help, I would not have been able to do this. Finally I want to thank Jesus Christ, my Lord and Savior. There are no words to describe the debt that I owe. Amen.

TABLE OF CONTENTS

LIST OF FIGURES

LIST OF ABBREVIATIONS

ECM	Extra cellular matrix
FN	Fibronectin
MIDAS	Metal ion dependent adhesion site
ADMIDAS	Metal Ion binding site adjacent to MIDAS
EM	Electron microscopy
tr$\alpha_5\beta_1$-FC chimera	truncated $\alpha_5\beta_1$-FC chimera
m$\alpha_5\beta_1$	Membrane supported $\alpha_5\beta_1$ integrin
s.e.m.	Standard error of the mean
RGD	Arginine-glycine-aspartic acid
BFP	Bio membrane force probe
RBC	Red blood cell
LFA-1	Leukocyte function associated antigen 1
ICAM-1	Intercellular adhesion molecule 1
AFM	Atomic force microscope

SUMMARY

Cellular adhesion plays a crucial role in the biological function of cells, allowing them to communicate and signal, as well as physically anchor, by enabling them to adhere to either other cells or the extra cellular matrix (ECM). This process is regulated by several factors including intrinsic bond kinetics, internal cellular signaling, environment, force exerted on the bond, and force history of the bond. Concerning the force and force history dependence, the observation of catch bonds in integrin binding has asked as more questions than it has answered.

To explore the force and force history dependence this process, each bond was loaded to a peak force before relaxing to a much lower force that was held for the duration of the measurement. Two different integrins were studied, both of which have in previous works exhibited a catch bond. Furthermore, the effects of different metal ion conditions and an allosteric antagonist were also studied to elucidate the conformational effects on force priming of integrin. What was observed was that I domain, or αA domain, possessing integrin, whether tested against its more active or less active binding state, changed very little in terms of off rate once the priming force was applied. However in the I domain, or αA domain, lacking integrin, the observed off rate changed as well. It seems that force priming is capable of causing integrin to bind in a stronger manner regardless of the other conditions used to either activate or inhibit binding. However the way in which the binding is strengthened depends on the receptors structure.

CHAPTER 1

SPECIFIC AIMS

The following objectives were proposed to study force activation effects on ligand binding to integrins both possessing and lacking an I domain, or αA domain.

1. Characterize the bond lifetime-force relationships of integrin $\alpha_5\beta_1$ and fibronectin interaction in the force primed and unprimed cases.

$\alpha_5\beta_1$ binds fibronectin on the cellular surface and this bond, in physiological conditions, is constantly under stress. Previous work on this interaction has revealed a catch bond [27]. However, the mechanism for this is currently unknown. One area of debate regarding this phenomenon is whether a large force is required for the duration of the bond to cause this. To understand this, $\alpha_5\beta_1$ expressed on live cells were brought into contact with a fibronectin fragment, FN $III_{7\text{-}10,}$ and the bond lifetime was measured under force. One set of measurements were performed after the bond experienced a ~20 pN priming force and the force was relaxed to, and held at, ~5pN. The other set of measurements were performed with force simply being held at ~5pN for the entire bond lifetime without experiencing a higher priming force. Previous work has shown force activation of $\alpha_5\beta_1$ before but used a FC chimera instead of a live cell [27]. This work, while important and extremely useful, does not demonstrate if this phenomenon can happen on a cell or if there is something about the way the cell controls its integrin that might prevent this.

Integrin conformation is controlled by several factors including signaling from inside the cell and the metal ions present outside the cell. It has been shown that different divalent cations cause a shift in conformation populations of the integrin and it is has been shown that integrin conformation is closely tied to integrin affinity [10]. To further understand the role of these ions play in force regulation of $\alpha_5\beta_1$/FN interaction, lifetimes were measured in media containing either 2mM concentration of magnesium/EGTA or manganese. From this we hope to determine if force activation is possible on the cell as well as what role conformation plays.

2. Characterize bond lifetime-force relationships of integrin LFA-1 and ICAM-1 interaction in the primed and unprimed cases.

Similar to the $\alpha_5\beta_1$/FN interaction, LFA-1 has also been shown to exhibit a catch bond when binding human ICAM-1 [28]. Previous work on cross species reactivity has shown that while mouse LFA-1 will not bind human ICAM-1; human LFA-1 can bind mouse ICAM-1 similar to what was used in the work presented here [52,53]. As LFA-1 also possesses an I domain, it was suspected that this receptor would behave differently from $\alpha_5\beta_1$ when the bond lifetime was measured after experiencing a priming event. Previous work has been done showing that catch bond behavior might be observed because of the change in affinity of the synergy site on $\alpha_5\beta_1$ when the receptor is under load [45]. While this is an acceptable explanation for a RGD integrin like $\alpha_5\beta_1$, LFA-1 has no such synergy site.

Again, since LFA-1 possesses an I domain, all ligand binding takes place away from the β propeller where the aforementioned synergy site is located. However, the I domain has been characterized as an endogenous ligand for the head piece of the integrin. Therefore, it is possible or even likely that if force priming does affect ligand binding in the I lacking case then it could affect it in the I possessing case. Additionally, testing an I domain possessing integrin on a live cell will allow us to know more thoroughly if this type of event is a common characteristic of all integrin types.

3. Investigate the effects of XVA-143 on force priming.

The specific residues and secondary protein structure where the bind is formed between the ligand and the integrin is known as the binding pocket. When dealing with integrin, the binding pocket can be said to exist in either an open or closed conformation with the open conformation associated with higher affinity binding. Since LFA-1 possesses an I domain, that is the location of the binding pocket for this type of integrin. I domain containing integrin are susceptible to a molecule known as XVA-143. The I domain is believed to be an intrinsic ligand for the I-like domain. XVA-143, a small molecule, is known to inhibit ligand binding in I domain possessing integrin by stabilizing the I-like domain in a high affinity conformation but preventing the I domain from binding to the I-like domain which correlates to a low affinity I domain binding pocket. XVA-143 effects binding to the I domain then by inhibiting the binding between the integrin headpiece and the I domain [1]. When this occurs the integrin legs and headpiece extend. This combination of an extended integrin with a low affinity

binding pocket is known as the intermediate affinity state. Therefore, by priming the integrin in the presence of XVA-143, the importance of the interaction between the I and I-like domains can be better understood with regard to binding strength and behavior under various loads and loading conditions. Also, the local conformational changes from this and the previous two specific aims can be used in concert to better understand how integrin activation occurs.

CHAPTER 2

BACKGROUND

The main load bearing receptor in mammalian cells is integrin. Integrin is responsible for a wide variety of physiological events such as tissue morphogenesis, cellular differentiation, wound healing, inflammation response, leukocyte trafficking, etc. Integrins are a large family of intercellular heterodimeric adhesion and signaling receptors. There are currently 24 known human integrins consisting of one of 18 types of α subunits and one of 8 types of β subunits [2]. There are 12 known integrin types that possess an extra portion, an approximately 200 amino acid structure known as the I domain, which exists on 8 types of α subunits; αL, αM, αX, αD, α1, α2, α10, α11 and αE as can be seen in figure 2-1. The two subunits are non-covalently bound and with the N-terminus of each meeting in a globular head that provides the binding site for ligands except when an I domain is present [3]. In that case, the ligand binds to the I domain. Each integrin subunit also has a cytoplasmic tail and a transmembrane portion. However, the extracellular portion of the receptor is much larger than the other two segments (figure 2-2).

Previous EM and crystallographic studies have reported various and conflicting conformations of integrins under different conditions. EM imaging showed what looks like an extended integrin with straight leg portions [7-9]. Later, crystal structures of $\alpha_V\beta_3$ showed a bent conformation [5,6]. EM imagining done by the Springer group in various metal ion conditions provided some resolution to this apparent conflict by showing a mostly bent conformation

population of integrin in the presence of calcium but an extended conformation in the presence of manganese [10]. This conformational change was also previously observed by a change in the Stoke's radius of integrin when in the presence of small ligands [11]. While alone these findings were very interesting, when considered with integrin's affinity dependence on the metal ion types present in the environment implied an allosteric relationship between the receptor's conformation and its affinity [10]. Given this data, a model for integrin unbending as it related to affinity and binding was proposed. The model stated that Integrin must open at the knee, or genu region, before binding could occur. This conformational change model is known as the switchblade model [12]. While this model is a cause of some debate in the field, it is the most widely accepted model to date.

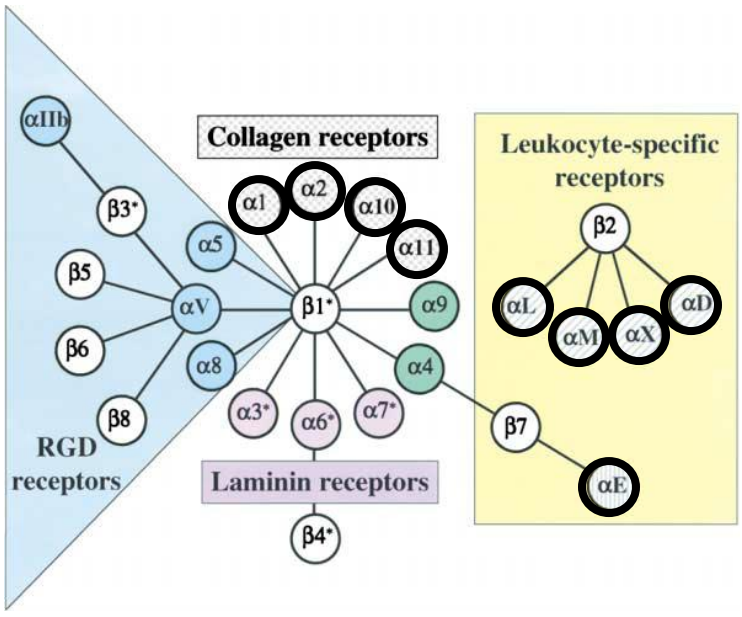

Figure 2-1. Integrin Receptor Family. The Integrin family of receptors is made up of 24 individual, heterodimeric pairs consisting of one α and one β subunit. Each integrin type is then shown as a line connecting the subunits. The α subunits highlighted with a dark circle signify α subunits that possess an I domain. Figure taken from reference [4].

As shown earlier, changes in the affinity relate back to allosteric, long range changes in the molecule. In the switchblade model there are two “pathways” which regulate these two changes, known as inside-out and outside-in signaling (figure 2-3)[15]. Inside-out signaling, capable of increase the receptors affinity as much as 1000 times, is the process by which the cell itself alters the affinity of the integrin through binding of the intra-cellular tails of the two subunits [4,14]. This causes an extension of the integrin as the headpiece and legs straighten. This is known as the intermediate affinity state. The separation of the legs can facilitate the larger scale conformational change and straightening of the leg portions as the headpiece breaks its interactions with the body. It is also believed that to reach the highest binding affinity, the legs and transmembrane segments must separate and the hybrid domain must extend out from the β subunit. The hybrid domain extension facilitates a conformational change in the I-like domain resulting in an increase in affinity in both I-like and I integrin [1,16]. In I-like integrin, meaning integrin lacking an I domain, as the hybrid domain separates from the β subunit, the α7 in the I-like domain helix is pulled down [10]. When the α7 helix shifts, it causes a rearrangement of the hydrophobic core which in turn causes a change in the position of the α1 helix. The α1 helix is important for positioning residues involved in coordinating the metal ion occupying what is known as the ADMIDAS site [17]. The ADMIDAS is then believed to help stabilize the I-like domain and regulate binding to the MIDAS site

which serves as an important ligand binding site by allowing a glutamate residue present on the ligand to coordinate with its metal ion [18].

I domain possessing integrins are activated in a similar fashion. The I domain is a GTPase-like domain with the catalytic site missing [16]. Instead, at the top of the domain is a metal ion site which serves as a primary ligand binding site in the same way the MIDAS site on the I-like domain [17]. The I and I-like domains are very similar when overlaid on top of each other [16]. However, among a handful of other differences, there is no ADMIDAS site on the I domain regulating the MIDAS site. Even in the absence of this, the shift from a low, or closed, to high, or open, conformation can be seen as very similar between the two, both involving their respective α1 and α7 helixes, particularly the downward shift of the α7 helix [19-21].

Outside-in signaling can be thought of as similar to outside-in signaling but in reverse. First the knees separate before the transmembrane segment and the binding of the ligand causes the hybrid to swing out as described earlier [15]. Outside-in signaling is initiated by ligand binding and allosteric and conformational changes in the molecule conceivably could prime the subunit tails for binding intracellular proteins.

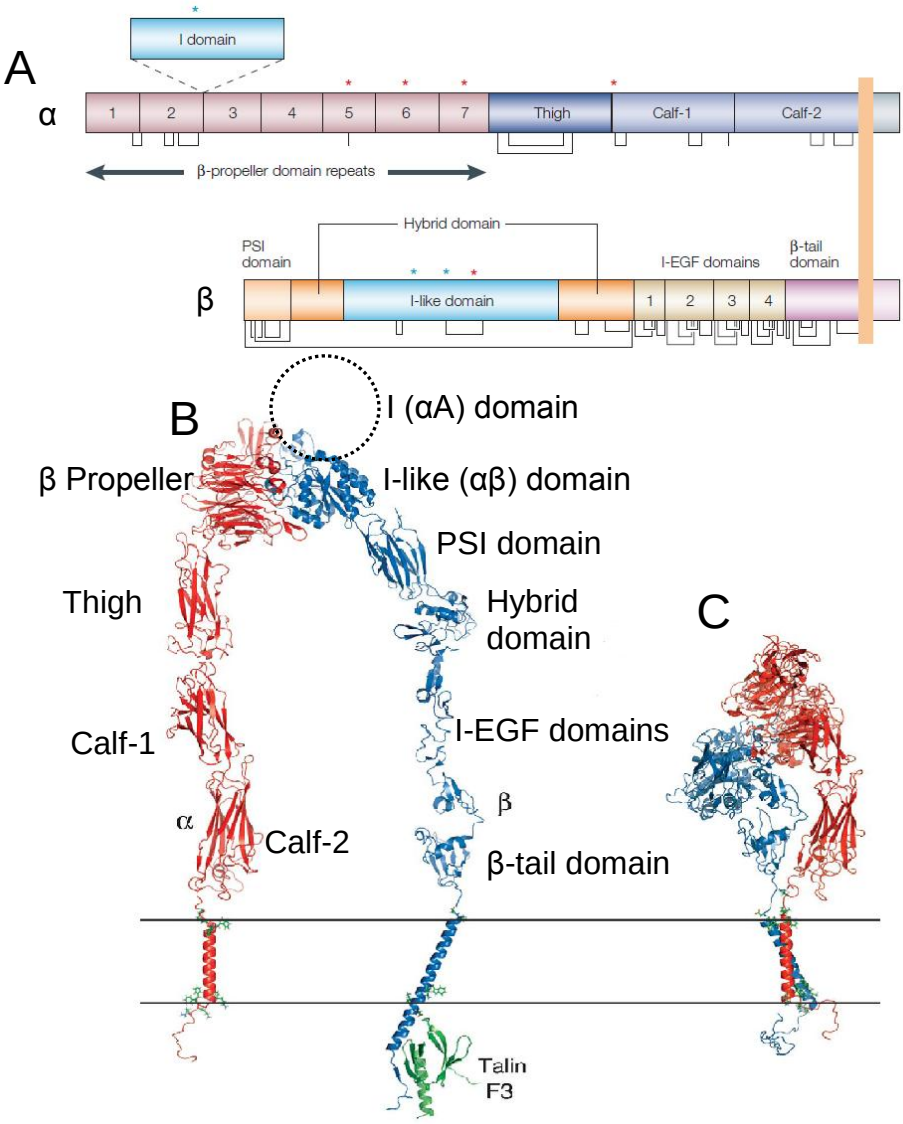

Figure 2-2. Integrin Structure. A) Primary structure of both extracellular portions α and β subunits [13]. B) Illustration of extended integrin subunits with α_{IIb} and β_3 transmembrane segments with the Talin F3 domain bound to the β subunit's intracellular tail. Each domain from (A) is shown with the exception of the I domain which is not present in the illustration and is represented by the dashed circle. C) The same integrin domains illustrated in the bent, inactive conformation. (B) and (C) are adapted from reference [14].

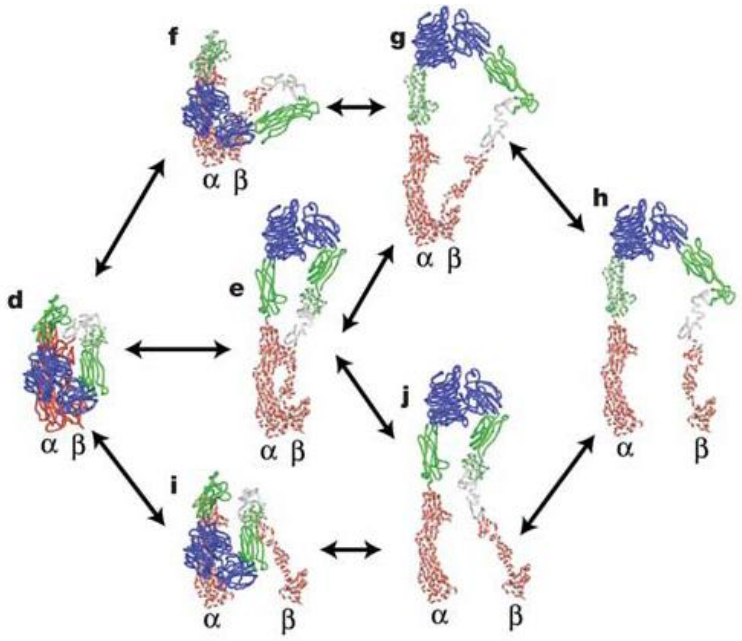

Figure 2-3. Proposed transition between conformational states. Outside in and inside out signaling as proposed in the switchblade model. Inside out signaling is the path from d to h through i and j. Outside in signaling is the path is from d to h through f and g [15].

The link between the ligand and cytoskeleton, facilitated by the integrin, is completed by what are called adaptor proteins, including talin, paxillin, vinculin, Shp2, filamen, and/or α-actin, which link the β tail of the integrin to the actin cytoskeleton [22]. It is also believed that cells can use force, through the binding of adaptor proteins, as regulated by the cytoskeleton, to control both integrin clustering and affinity. Myosin motor proteins can generate forces on the integrin bonds. The cell can form large adhesion complex involving ordered arrangements of integrin as well as other adaptor proteins and signaling molecules. In several cases it has been shown that force is required for stable adhesion formation and force has been reported to stabilize the high affinity conformation of the α7 helix I possessing integrin [23-25]. Some of these adhesion complexes have been shown to correlate the force exerted at the

adhesion site with the number of integrin involved as well as the orientation of the site [26]. Recently it has shown seen on a single molecule level with the observation of catch bonds between α5β1 and fibronectin as well as between LFA-1 and ICAM-1 meaning integrin-ligand bond lifetimes are prolonged by increasing force [27, 28]. As the affinity of the receptors increases, multivalent ligands such as fibronectin or ICAM-1 could feasibly cause clustering leading to an increase in the avidity of multivalent interaction. However, mechanical regulation of integrin binding does not have to be a signaling event because, in the absence of cytoskeletal control of the receptor, shear flow can also cause these effects [23].

α5β1, also known as VLA-5 (very late antigen-5) or CD49e/CD29, is a very important and often studied integrin receptor. It is an I domain lacking integrin that consists of a 114 kDa α subunit and an 84 kDa β subunit. α5β1 is important in leukocyte trafficking as well as a variety of other functions and is present on a number of different cell types throughout the body, such as osteoblast.

The main ligand for α5β1 is fibronectin. Fibronectin, an extracellular glycoprotein, is secreted in a soluble form and assembles into a fiber network on the surface of the cell. It is a dimer composed of two similar subunits and is made up of three different types of modular domains, type I, type II and type III. The main binding sites on fibronectin exist on the third domains between modules seven through ten (figure 2-4).

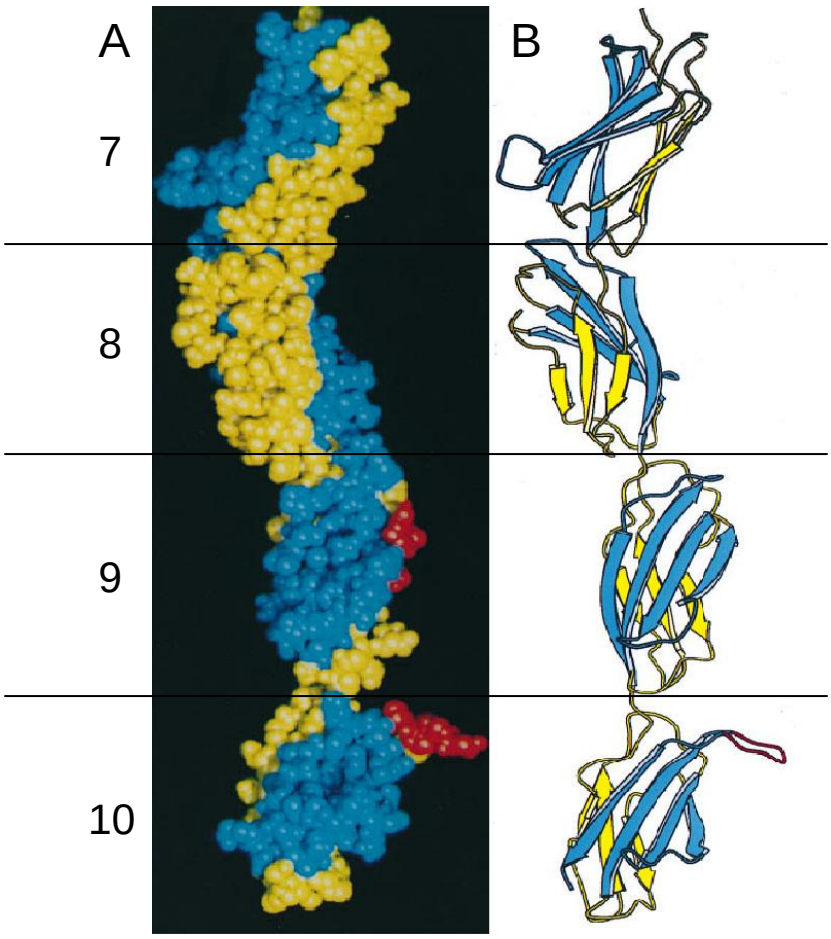

Figure 2-4. A space-filled and ribbon diagram of the FN III 7-10. A) A space-filled model of the crystal structure of the type III subunits 7-10. Each subunit is divided by a line and labeled on the left hand side of the figure. The red portions in subunits 9 and 10 are the synergy binding site and the RGD binding site respectfully B) A ribbon diagram of the space-filled model in (A). This model shows the secondary structure and orientation of the β sheets in each subunit (blue and yellow portions). This figure was adapted from reference [47].

On the cell surface, fibronectin forms long fibers that form a two dimensional network. As force is applied to the network, $\alpha_5\beta_1$ clusters which allow for larger adhesion sites to form [50]. Increased and decreased fibronectin expression has been linked to cancer growth as well as defects in neural tubes and vascular development.

αLβ2, also known as LFA-1 (lymphocyte function associated antigen-1) or CD11a/CD18 is another very important immunological receptor. It contains an I domain (figure 2-5) as its only ligand binding site and exists as part of a larger family of leukocyte integrin, all of which contain a β2 subunit. αLβ2 is important for T lymphocyte immunological synapse formation as well as leukocyte trafficking. Deficiencies in the expression of LFA-1, as well as other leukocyte integrins, have been linked to a condition known as leukocyte adhesion deficiency which results in decreased resistance to infection [48].

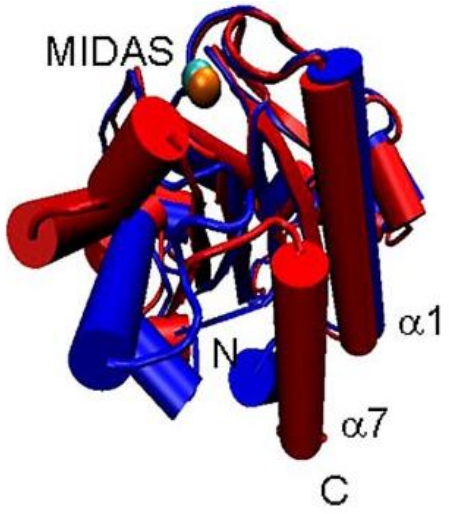

Figure 2-5. I domain. An I domain from an α_L subunit. The locked open (blue) and WT closed (red) domains are both represented in this overlay with a manganese ion in the MIDAS position [29].

αLβ2 binds I-CAM-1, ICAM-2 and ICAM-3 as well as ICAM-4 and ICAM-5, although the physiological basis for these is unknown. Of these though, the primary ligand for αLβ2 is ICAM-1 which mediates a significant portion of known leukocyte functions. ICAM-1 is a 90 kD surface glycoprotein that promotes inflammatory and immunological adhesion. Belonging to the immunoglobulin

family of molecules, ICAM-1 consists of four domains, each approximately the same size as a typical Ig domain, and a fifth truncated domain as well as a small transmembrane domain and a small intracellular portion that binds to the actin cytoskeleton. ICAM-1 exists as a dimer on the cell surface. ICAM is expressed at low levels on some cell types such as endothelial and T cells but can be forced to express higher levels on many more types if induced through one of a variety of signal types, i.e. cytokines, shear stress, etc.

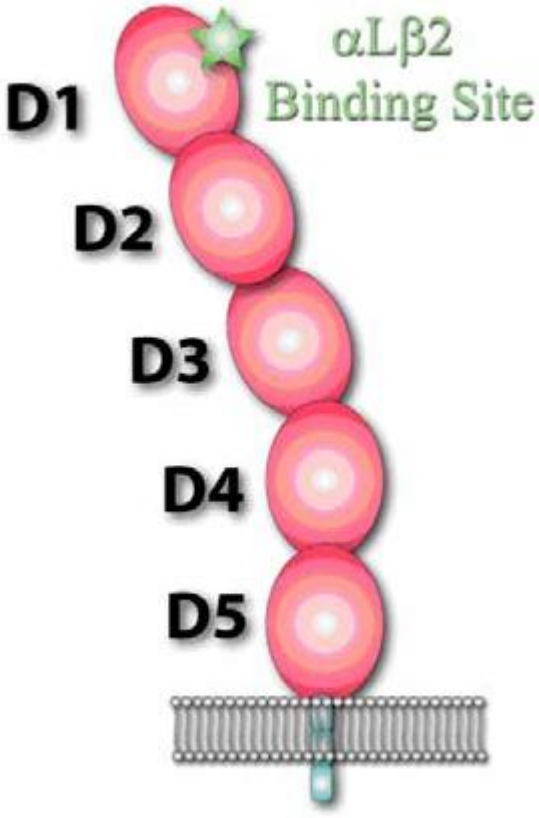

Figure 2-6. Drawing of ICAM-1 monomer. [28]

Receptor-ligand interactions, such as those observed between $\alpha_5\beta_1$ and fibronectin or LFA-1 and ICAM-1, are governed by simple, reversible chemical reaction kinetics. In this framework, two concentrations, brought into contact with

each other have a “forward” rate k_f which is the rate at which the two molecules associate, receptor R and ligand L, join to form a third complex C. Likewise, they also have a “reverse” rate k_r, which is the rate at which that the parts of the complex C disassociate from one another and return to the original components, R and L. The two rates are also known as on-rate and off-rate respectively. This can be written as [30]:

$$R + L \underset{k_r}{\overset{k_f}{\rightleftharpoons}} C \qquad \text{Equation 1}$$

Which can be rewritten as the differential equation:

$$\frac{d[C]}{dt} = k_f[R][L] - k_r[C] \qquad \text{Equation 2}$$

Under this model, the concentration of C will reach an equilibrium state after a long period of time. At that point the concentrations of the three stabilizes and the amount of C produced equals the amount of C destroyed. When this occurs, what is known as the affinity K_A can be expressed as:

$$K_A = \frac{k_f}{k_r} = \frac{[C]}{[R][L]} \qquad \text{Equation 3}$$

This is a much idealized case. This kinetic framework was created to characterize three dimensional molecular binding where the components are suspended in a fluid. However, a significant portion of cell receptor binding takes place in two dimensional cases where the individual binding components are fixed on a surface. Furthermore, when this geometry is considered, the bonds formed exist under a load which can have a significant effect on the off-rate involved. Under these circumstances, normally it would be expected that the

bond would disassociate faster with the application of greater forces. However this is not always the case. Currently there are two ways of describing how reversible bonds are affected by force: slip bonds and catch bonds.

Slip bonds are exceedingly common. They are considered the standard model for reversible binding under load and include streptavidin-biotin as well as antibody-antigen reactions [31, 32]. In the slip bond case, as outlined in what is known as the Bell Model, the bond lifetime will decrease exponentially with increasing force [33]. As the force increases the energy barrier that separates the bound and disassociated states decrease and the likelihood of a transition between the two becomes more likely [30]. In this case k_r was described by Bell as:

$$k_r = k_r^0 e^{\frac{-E_b(f)}{k_B T}} = k_r^0 e^{\frac{-f x_\beta}{k_B T}} = k_r^0 e^{\frac{-f}{k_b T / x_\beta}} = k_r^0 e^{\frac{-f}{f_\beta}} \quad \text{Equation 4}$$

This is a mathematical relationship between the off rate, the unstressed off rate k_r^0, and the energy barrier E_b separating the bound and unbound states. The energy barrier is a function of the force *f*, and the width of the energy barrier x_β which, taken together, are used to calculate the total work needed to overcome the energy barrier. The other factors involved are the Boltzman constant, k_b, the absolute temperature, T, and f_β, a scaling factor in force units that relates the Boltzman constant and the temperature to the energy barrier.

Catch bonds are far rarer. These types of bonds exhibit a counterintuitive behavior where an increase in the force experienced by the bond results in a longer-lived bond [32, 35]. The mechanism for this is very specific to the structure

of the molecules in question. Thus far catch bonds have been observed in selectin/ligand interactions [32, 56], glycoprotein Ib and von Willdebrand factor interactions [36], myosin/actin interactions [51], the bacterial FirH receptor and mannose [37] and recently has been observed between purified α5β1 and fibronectin[27] and between LFA-1 and ICAM-1 [28].

For either type of bonds, the parameter being studied is the off rate since both cases related to bond disassociation. One way of measuring the off rate of a bond is done by measuring a large number of bond lifetimes. A bond lifetime is the amount of time a bond lasts under a given force. For any given force, the lifetime distribution can usually be modeled as an exponential relating the bond lifetime to the bond's off rate as expressed as [32]:

$$P_a = e^{-k_r t} \qquad \text{Equation 5}$$

Where "t" is the lifetime of the bond and P_a is the probability that a bond will last for that amount of time. Using this model, plotting the natural log of the number of measurements order against the bond lifetime will show a line which has a slope equal to the off rate. This is accomplished practically by ordering the lifetimes from longest to shortest and assigning each lifetime a number x between 1 and n, where n is the total number of lifetimes measured. The longest lived bond being assigned 1 and the shortest n. Taking the natural log of x for each and plotting that against its corresponding lifetime should yield a data set which can be fit linearly.

Quantifying the force-lifetime relationship for cell receptors has been a difficult proposition. Initially, adhesion complexes were observed between cells

and ligand coated substrates by studying migrating cells or in flow chamber experiments. However the complex and often unknown nature of the mechanical and kinetic behavior of the cells, cellular components and individual molecules involved limited the amount of information that could be taken from these experiments in terms of the individual response of receptor-ligand binding pairs. To overcome such limitations several single molecule techniques have been developed to address these issues.

Adhesion frequencies in these techniques are usually kept very low (<20%) to ensure the vast majority of bonds are single receptor ligand pairs as understood in previous work [54]. Using this methodology, a number of single molecule techniques have been developed using very soft spring constant transducers to measure deflections and forces. They are the atomic force microscope (AFM), magnetic tweezers (MT), optical tweezers (OT) and the bio-membrane force probe (BFP).

The AFM operates by bringing a tip mounted on a soft cantilever into contact with a substrate [32, 38]. The cantilever is then retracted and the deflection of the cantilever is found by measuring the change in position of a laser spot from a beam that is reflected off the back of the cantilever. Usually the tip and substrate are coated in the two molecules being tested. This technique is considered the easiest of the single molecule techniques to run but has difficulty measuring the very low force events due to the relatively high spring constant of the cantilever.

MT's and OT's both operate in a similar fashion to each other. Both use either a very finely focused laser or a magnetic field as a trap to hold either a magnetic or glass bead in a certain position by creating an energy well whose restoring force maintains the bead at a center position [39,40]. The bead is then brought into contact with either another bead or a cell held in a similar trap or aspirated into a micropipette and manipulated using a piezo-electric manipulator. The two particles are brought into contact and then separated. If there is a bond between the two, then a change in position will be measured. These two techniques offer the lowest spring constants but are also the most difficult to set up and run. Additionally, the laser can kill cells used in the experiment and can be very dangerous due to the extreme power output required.

The final technique, and the one used for this study, is the BFP (figure 2-7). The BFP uses an over-inflated red blood cell (RBC), aspirated into a stationary micropipette, as a force transducer [28, 30, 42]. A glass bead coated with the ligand of interest is then placed on the red blood cell and brought into contact with the "target", usually another bead or cell which is aspirated into a micropipette and controlled by a piezo-electric manipulator. As the target is retracted, the deflection of the glass bead can be measured by a high speed camera and a computer. The image of the glass bead is analyzed by a program which fits a profile of a dark circle around the glass bead. Using this profile a very accurate bead position can be found by constantly finding the center of the black ring. Assuming linear motion in a plane perpendicular to the line of sight of the camera, this technique is exceedingly useful because of the accuracy and

sensitivity of the method as well as the ease of using either protein coated beads or whole cells.

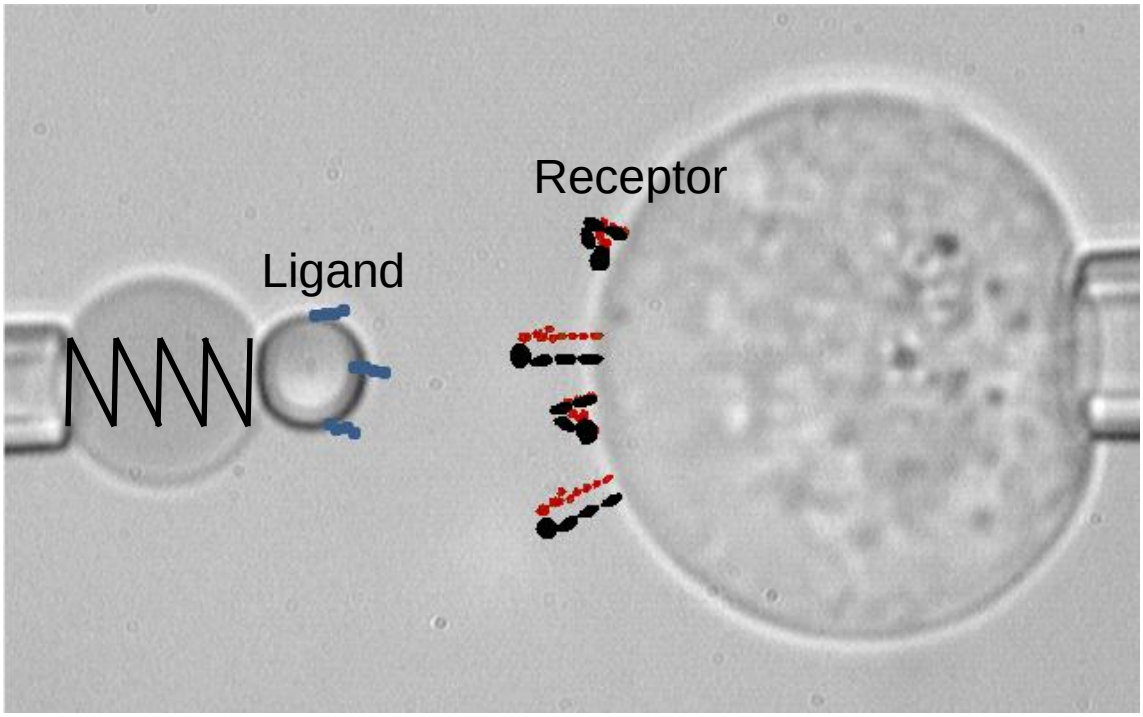

Figure 2-7. BFP setup. The BFP setup as taken during an experiment. From left to right. The aspirated RBC as a force transducer, the attached glass bead coated in ligand and the aspirated cell expressing the receptors of interest.

Using some of the methods described above, work has been done on the force/binding relationship between integrins and their lignands. Kong et. al. investigated the force regulating effects on $\alpha_5\beta_1$-FC chimera on an AFM using the same ligand used later in the BFP experiments presented here [27]. Initially, this experiment explored the possibility of a catch bond between the fibronectin fragment and the integrin chimera under the following conditions; calcium/magnesium, magnesium/EGTA and manganese. The catch bond under these conditions did change in characteristic but was never abolished (fig.2-8). Unfortunately it cannot be known how different these conditions were as the

maximum measureable force in this experiment was limited by the capture antibody slip bond, as seen in the gray data points (figure 2-8). Metal ion condition in that experiment was examined in light of the overall integrin conformation. Calcium/magnesium generally have a more bent integrin population while manganese has a more extended population. Magnesium/EGTA is believed to be somewhere in between the two. If the catch bond never disappeared then the longer lifetimes observed is not a result of a increase in affinity caused by a global conformational change.

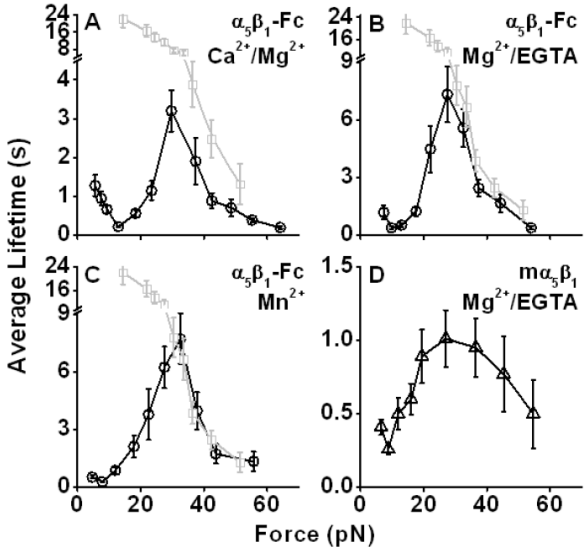

Figure 2-8. Catch bond in purified molecule system. Plots of the average lifetime versus the force under which those lifetimes were measured in the presence of different metal ion conditions. The grey data points in [A-C] are the capture strength of an antibody used to attach the $\alpha_5\beta_1$-FC to the AFM tip. [D] is a different experiment done on whole integrin supported in a lipid bilayer. The error bars are s.e.m. Figure taken from reference [27].

In fact, it appears that the actual process of extension has little to no effect on the catch bond. Also in the $\alpha_5\beta_1$-FC chimera study, a truncated chimera was used that was only the $\alpha_5\beta_1$ head piece. Using this molecule, no extension is

possible. This time however, the catch bonds remained and surprisingly were unaffected by the metal ion condition (figure 2-9). Clearly, truncated integrin receptors seem to exhibit greater activation potential related to force.

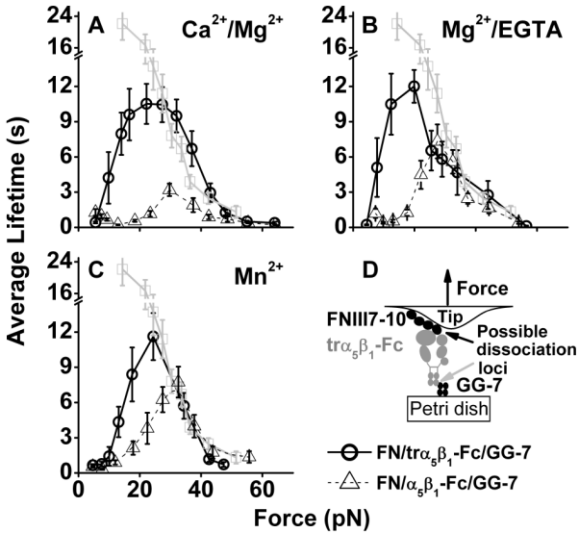

Figure 2-9. Catch bonds of truncated $\alpha_5\beta_1$-FC chimera. The light gray line in each figure represents the dissociation of the antibody used to capture the $\alpha_5\beta_1$-FC chimera on the Petri dish. All error bars represent s.e.m. The circle data points signify the truncated $\alpha_5\beta_1$-FC chimera lifetime data while the triangular data points represent the full length $\alpha_5\beta_1$-FC chimera lifetime data. [D] is a drawing of the experimental setup used for this experiment. Figure taken from [27].

Finally, previous work examined a force priming effect on binding between both the full length and truncated chimeras and the fibronectin fragment. Force priming did indeed have a significant effect on the average lifetime of the bond (figure 2-10). There was not a drastic difference between the lifetimes observed according to metal ion condition but the magnesium/EGTA condition did show a noticeably longer average lifetime than the manganese condition (figure 2-10). Additionally, the average lifetime increased even further with a truncated $\alpha_5\beta_1$-FC chimera (figure 2-11). When whole, membrane supported integrin was used a

drastic increase was also seen but not to the extent as seen with the in that chimera experiments (figure 2-11).

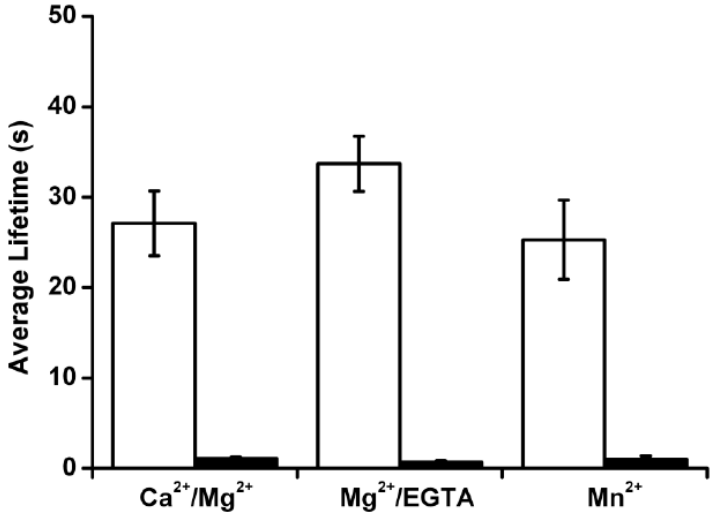

Figure 2-10. Average with and without priming of purified molecules. The solid bars signify the unprimed case while the white bars signify the primed case. The error bars represent the s.e.m. Figure taken from [27].

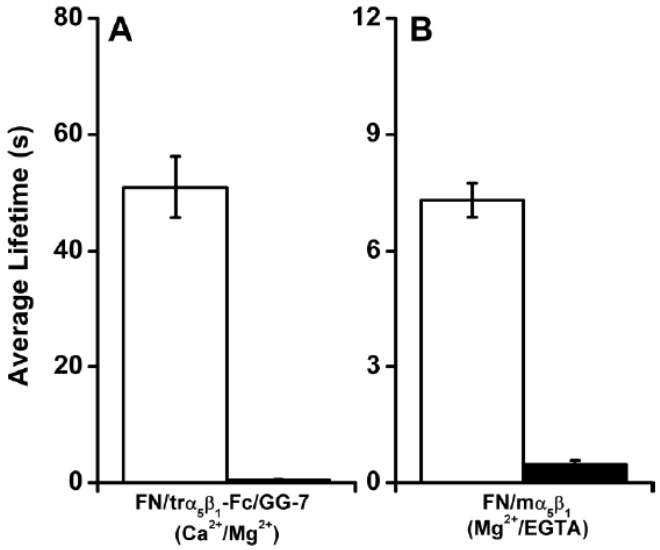

Figure 2-11. Average lifetimes of truncated and membrane supported integrin molecules under force primed and unprimed condition. The solid bars signify the unprimed case while the white bars signify the primed case. The error bars represent the s.e.m. (A) lifetime data using a truncated $\alpha_5\beta_1$-FC molecule. (B) lifetime data from whole integrin supported in a lipid bilayer. Figure taken from [27].

Similar to the above AFM experiment, the force lifetime relationship was studied using human ICAM-1 and human cells expressing LFA-1 on the BFP [28]. The primary focus of this study was to investigate the presence of a catch bond similar to the $\alpha_5\beta_1$ catch bond. What was determined, as can be seen in figure 2-12, is that there was indeed a catch bond for this receptor. And, as seen in the $\alpha_5\beta_1$ experiment, it changed in terms of some of the characteristics that describe it but was never abolished by metal ion condition.

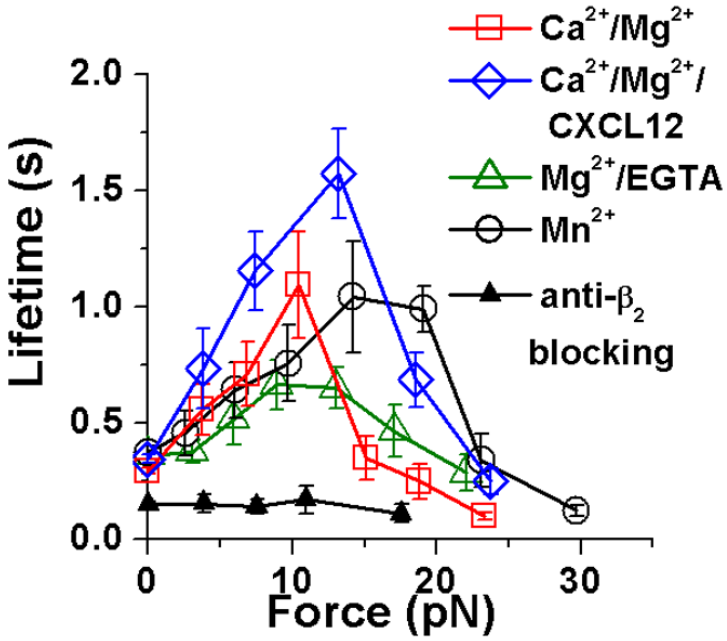

Figure 2-12. Force lifetime relationship for human LFA-1/ICAM-1. [28]

The force binding relationship for this bond was also measured in the presence of XVA-143. XVA-143 is a small molecule inhibitor known to bind to the LFA-1 headpiece. XVA-143 has three significant effects on the conformation of LFA-1 which strongly affects it ability to bind ligand. The first effect XVA-143 has is to shift the global conformation of the integrin to an extended, leg separated

state. Also, the α7 helix in the I-like, or βA, domain shifts to its lower position. In I domain lacking integrin, the α7 helix in its lower position in the I-like domain is characteristic of open headpiece. Similarly, extended integrin with its leg portions separated is normally associated with high affinity integrin. The inhibitory effect of this molecule then is associated with its third significant conformational change; XVA-143 blocks association between the I-like domain and the I domain. This, in effect, places the I domain in its closed conformation that is no conducive to strong ligand binding. The effects of this, with regard to the previous work done on LFA-1, is the abolishment of the LFA-1/ICAM-1 catch bond (figure 2-13).

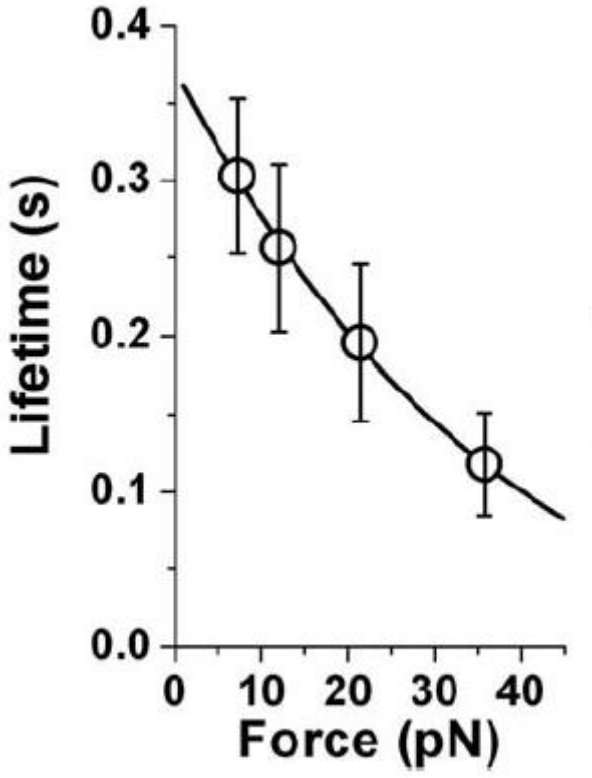

Figure 2-13. Lifetime of LFA-1-ICAM-1 in the presence of XVA-143. Constant force versus lifetime measured in the presence of XVA-143. Taken from reference [28].

CHAPTER 3

MATERIALS AND METHODS

Isolation of Human Red Blood Cells (RBCs)

Human RBCs were isolated from a fresh whole blood obtained by a finger prick. The RBCs were washed three times in the carbonate/bi-carbonnate buffer (pH 8.4, ~180 mOsm) in a centrifuge set to 2000 RPM for 30 seconds. Finally the RBC pellet from the third wash was covered with 100µl carbonate/bi-carbonate buffer for protection while the biotinylation solution was prepared of RBCs. Once the reagents were ready, the RBCs were incubated in a 6 mM NHS-PEG-biotin solution for 30 minutes before being washed twice in carbonate/bi-carbonate buffer and once with 300nM Hepes solution. The biotinylated RBCs were then stored in 50 ul of 300 mM Hepes solution in a refrigerator.

Culture of K562 cell line

Human erythroleukemia cell line K562 was purchased from ATCC (American Type Culture Collection). The cells were cultured in RPMI with 10% fetal calf serum with L-glutamine (4mM) and penicillin/streptomycin (0.1mg/ml). Maximum cell densities were ~$5x10^5$/ml.

Culture of Jurkat cell line

Jurkat cells, a cell line isolated from a patient with acute leukemia, was purchased from ATCC (American Type Culture Collection). The cells were

cultured in RPMI with 10% fetal calf serum with L-glutamine (4mM) and penicillin/streptomycin (0.1mg/ml). Maximum cell densities were ~5x10^5/ml.

Coupling of biotin onto RBCs

Biotinylation of RBCs was used to link the RBC to a streptavidin-coated glass bead. To biotinylate the RBCs, whole blood was gathered from a finger prick and washed 3 times (2000g, ~30 seconds) with carbonate/bi-carbonate buffer (pH 8.4, ~180mOsm). 2~3mg of the hetero-bi-functional polymer of SA-PEG-Biotin (MW ~3500Da, JenKemUSA, TX) was measured and mixed with carbonate/bi-carbonate buffer to make a 6mg/ml concentration PEG polymer solution. Next, 50 µl of polymer solution was quickly mixed with 3µl of the RBC pellets and 847µl of carbonate/bi-carbonate buffer. This mixture was incubated for 30 minutes at room temperature on a rotator to prevent the RBCs from settling on the bottom of the tube. After incubation, the RBCs were then washed twice with carbonate/bi-carbonate, and then once with Hepes buffer (pH 7.4, ~300mOsm). For storage the RBCs were re-suspended in 100µl of Hepes buffer (pH 7.4, ~300mOsm) and kept in a refrigerator.

Silanization of glass beads

In order to link protein conjugated with streptavidin onto glasses beads, the beads first needed to be silanized. The glass bead's surface needed to be modified from hydrophobic to hydrophilic in order to enhance the protein's coating efficiency. For this, glass beads (5mg) were washed with a boiling

mixture of 0.5 ml of H_2O_2 (30%) and 9.5 ml of NH_4OH (99%). Glass beads were then cooled by washing in 50ml of deionized water (dH2O) before being washed three more time with methanol (99%) and re-suspended in 100µl methanol (Sigma). After washing, the beads were incubated in a 50ml of solution consisting of 1ml dH2O, 48.1 ml methanol, 1.5ml MTPMS and 5 ml acetic acid (99%) (United Chemicals) on a rotator to prevent the beads from settling. Once the beads had incubated for 3 hours at room temperature, they were washed three more times with methanol before being resuspended in 500µl of methanol. This 500µl bead solution was divided equally into glass vials for drying. Dry argon was then blown into each vial before being placed an oven pre-heated at 120 ˚C for five minutes. All the vials were placed into a vacuum desiccators wrapped in aluminum foil and allowed to sit overnight to cool.

Coupling proteins onto glass beads via biotin-streptavidin bonding

Streptavidin-malimide (Sigma) was covalently linked to the surface of silanized glass beads in the following steps. First, streptavidin-malimide solution (66.7uM) and silanized beads were mixed together with PBS buffer (pH~6.8) at room temperature, and then incubated on a rotator overnight which kept the beads suspended in the solution. After the incubation, the mixture was washed with PBS buffer (pH~6.8) twice and once with Hepes buffer (pH ~7.4, 150mOsm). Then streptavinidated glass beads were incubated with the biotinylated proteins (i.e., biotinylated fibronectin fragments or biotinylated mouse ICAM-1) for 30 minutes at room temperature on a rotator to prevent the beads from settling. The

fibronectin fragment used was type III consisting of only the 7-10 domains with one biotin molecule attached on the end. The mouse ICAM-1 molecule used was mouse ICAM-1 dimer/FC chimera (R&D Systems) biotynilated with a commercial kit (Thermal Scientific). Following the incubation, the beads were washed three times in Hepes buffer (pH~7.4) before being resuspended in Hepes buffer (pH~7.4).

The BFP system

The BFP system uses a biological inverted microscope with 40X/0.75 objective lens (Zeiss). The BFP uses a biotinylated, aspirated human RBC, swollen under hypertonic conditions (150 mOsm), as a force transducer. A probe bead, which was earlier coated with streptavidin and biotynilated protein, was attached to the apex of RBC by a micro pipette controlled by a pneumatic micromanipulator. The force exerted on the RBC was determined by multiplying the linear change in position of the glass bead and the spring constant of swollen RBC. The deformation of the RBC was measured by tracking the edge of the probe bead with a high-speed camera (Prosilica, Cooke). The spring constant of the RBC was estimated using Evans' spring constant model. This spring constant is determined by the radiuses of the RBC and probe pipette, and the contact area between the glass bead and the inflated RBC under zero force. The cell expressing the desired integrin (i.e. K562 or Jurkat) was aspirated on the target pipette. The target pipette's movement was precisely controlled by a piezo electric manipulator controlled with a computer.

Measurement of binding frequency

To measure binding frequency, the target cell was driven by a piezo electric manipulator to contact the probe bead and then retract. When retracted, adhesions were detected by the observation of the movement of the glass bead in the direction of the target cell past the zero force position of the bead. The contact and retraction cycle described here was repeated between 50 and a 100 times to generate a sequence of binary values, 1 signifying an adhesion and 0 signifying no adhesion. The adhesion frequency was calculated by adding the binary values and dividing by the total number of contacts per bead/target cell pair. These binding frequency measurements were repeated on no less than 5 pairs of probe beads and target cells to obtain the average adhesion frequency.

Measurement of nonprimed bond lifetimes

The receptor-ligand dissociation kinetics were characterized by measuring the lifetime of the bond under a given force with the BFP. A lifetime experiment consisted of the following steps. A cell expressing the receptor if interest (i.e. LFA-1 or α5β1) was aspirated by the target pipette and brought into contact with the beat coated with biotynilated. The impingement of the glass bead/RBC denoted contact. The contact force and time were controlled by a computer. At the end of the contact time, the piezo electric manipulator then retracted the target cell away from the probe bead to a fixed distance. An axial deformation of the RBC toward the target pipette signified an adhesion. This deformation was

detected by a high speed camera. When an adhesion took place, the fixed distance created a constant mean force experienced by the bond. When no adhesion took place, the glass bead returned to its zero force position. With the BFP accuracy of 1-2 pN, the mean force was found by comparing the zero force position and the fixed, loaded position of the bead. The lifetime of the bond was measured from the time the piezo electric manipulator stopped retracting until the target cell dissociated from the probe. If the bond lasted longer than ten seconds then the target cell was sharply retracted until the bond dissociated. The above cycle was repeated to obtain a data set consisting of a large number of adhesion lifetimes. The mean force was held at ~5 pN for all lifetime measurements. Lifetimes were measured until the number of data points was sufficient to show a well-defined, linear region on the natural log plot of the bond number.

Measurement of primed bond lifetimes

Primed bond lifetimes were measured in a similar fashion as the nonprimed lifetimes with one difference. After the contact duration, the target cell was withdrawn to a large priming force, 20 pN for $\alpha_5\beta_1$/fibronectin fragment measurements or 15 pN for the LFA-1/ICAM-1 measurements). After this, the target was then moved back to the low force (~5 pN) at which lifetimes were measured. The bond was measured from the time the bond reached the low force to the time the bond dissociated or the ten second cut off was reached at which time the piezo electric manipulator was retracted sharply until the bond ruptured (fig. 3-1).

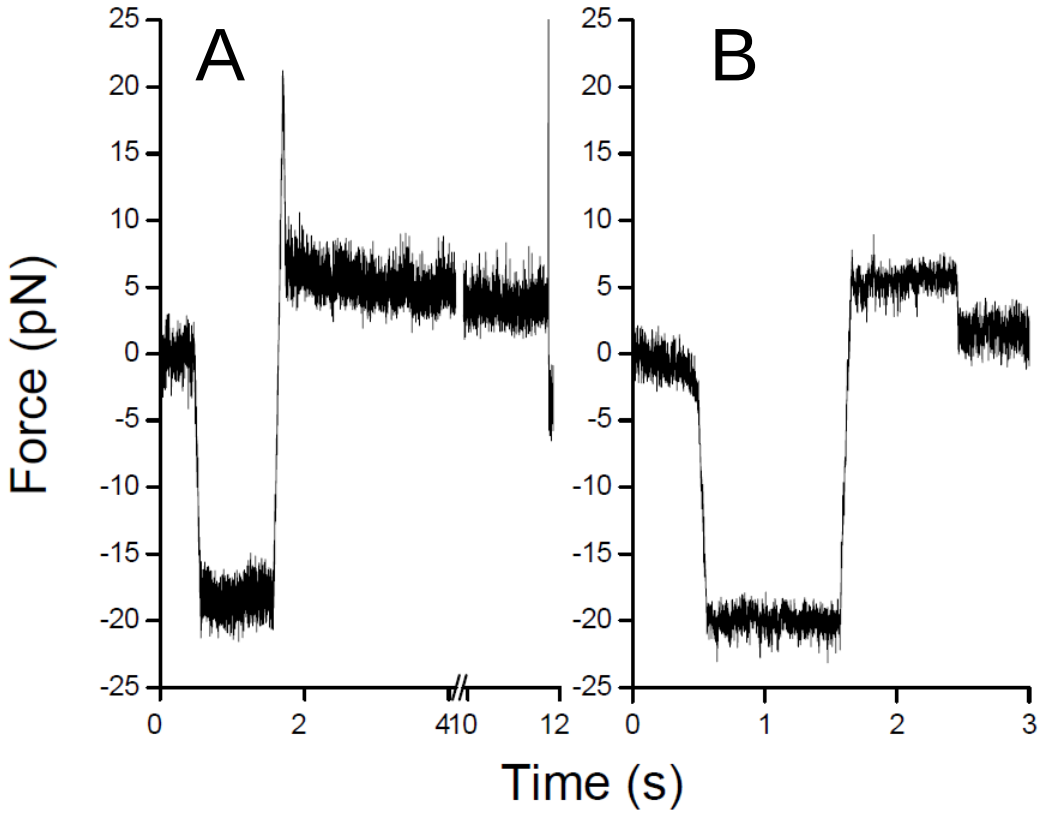

Figure 3-1. Force trace. A force trace of a primed event that went to the 10 second cutoff (A) and a non primed lifetime that spontaneously disassociated (B).

CHAPTER 4

RESULTS

Generally speaking, force priming did significantly increase the expected bond lifetime in all cases. The percentage of bonds that lasted until the ten second cutoff increased with priming for both types of integrins regardless of metal ion condition. Likewise the presence of an allosteric inhibitor did not nullify the priming affect.

Force-Priming Effect on I Domain Lacking Integrin

Before the other experiments were done, a series of controls were performed to demonstrate specific binding between $\alpha_5\beta_1$ and the fibronectin fragment. First the adhesions frequency of a K562 cell and a bead coated with streptavidin but no fibronectin fragment was measured to quantify amount of nonspecific interactions to be expected. After that, a similar test was performed to measure the adhesion frequency between the cell and fibronectin fragment coated bead in the presence of the antibody HFN 7.1, an antibody known to block the binding site on the fibronectin fragment used by $\alpha_5\beta_1$. This was done to determine if the adhesions measured in the experiment were in fact bonds between the fragment and the receptor. As expected, the adhesion frequency of both of these tests fell below the adhesion frequency measured when the actual experiment was run (figure 4-1). Also, given the observed behavior of the bonds under load, it is very unlikely that nonspecific binding could be responsible for the following results.

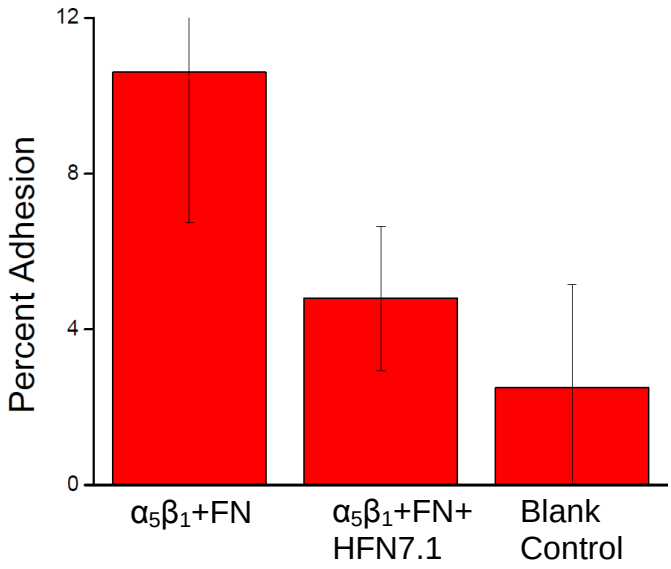

Figure 4-1. Adhesion percentage of $\alpha_5\beta_1$ experiment and controls. The adhesion frequency measured for each condition.

The specific aim put forth in this section of this work sought a similar goal to the purified molecule experiment described in the background [27] as well as to examine the physiological relevance of the previous results. The force priming seen in previous experiments were then investigated on living cells using the BFP. Live K562 cells, which have been shown not to express any other fibronectin receptors beside α5β1 [57], were brought into contact with glass beads coated with a fibronectin fragment. As was hypothesized, the expected bond lifetime increased after the bond was loaded to a force similar to the force at the peak lifetime in the previous work [27]. The previous, purified molecule study found a catch bond at approximately 30 pN no matter the metal ion conditions. However, for this experiment a priming force of 20 pN was used because of the K562 cells' tendency to form tethers. A tether forms when the cell receptor dissociates from the adaptor proteins or cytoskeleton before the ligand/receptor bond ruptures thus and changing the loading characteristics.

When a tether forms, large movements of the target cell results in very small changes in the force experienced by the bond.

After the bond was loaded to 20 pN, the force was relaxed to ~5pN for the duration of the lifetime measurement. In both metal ion conditions tested, magnesium/EGTA and manganese, the number of bonds that lasted past ten seconds increased considerably when compared to the unprimed case (figure 4-2).

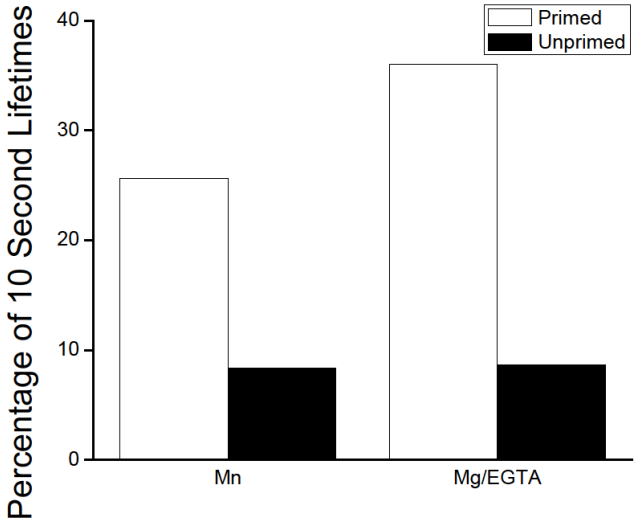

Figure 4-2. Percentage of lifetimes that last till the 10 second cutoff. The percentage of total lifetimes for each metal ion condition used in the $\alpha_5\beta_1$ experiment that lasted until the bond reached the ten second cutoff and was mechanically ruptured.

The lifetime distributions measured from experiments with and without mechanical priming in both the magnesium and manganese conditions are shown in figure 4-3 as semi-log plots. Because of the ten second cut off, the number of measurements will line up vertically. Nevertheless, inclusion of these data points gives rise to slopes for the data with lifetimes less than ten seconds, which represents off-rates of the subpopulations of bonds under the lines. The

data, as seen in figure 4-3, was then fit using a dual off-rate model based on equation 6.

$$P_a = Se^{-k_{r1}St} + Le^{-k_{r2}Lt}$$ Equation 6

The fit equation was found by taking the natural log of equation 6. This model contained four parameters, three of which were independent. The parameters were the fast off-rate, $k_{r1,}$ slow off-rate, $k_{r2,}$ fast off-rate fraction, S, and slow off-rate fraction, L. Since the total number of lifetime events remained constant for each case, the sum of the two fractions must equal one. Understanding that, the slow off-rate fraction was treated as the dependent parameter. From this fit, a value for both off-rates and fractions was obtained. From this fit, the fast off-rate is the parameter that dominates the initial, most steeply sloped, portion of the curves shown in figure 4-3. Likewise, the slow off-rate is the parameter that governs the next, more gently sloped, phase of the curves seen in figure 4-3. The two off-rate fractions then control how much influence either of the two off rates have on the overall shape of the curve. For example, a high slow off-rate fraction would increase the effect of the slow off-rate when determining the shape of the curve.

The magnesium/EGTA condition showed two off-rate distributions for both the unprimed case and the primed case (figure 4-3). The negative slope, which is a representation of the speed of dissociation or off-rate, was significantly lower with the application of a priming force than without a priming force, indicating that force priming slowed bond dissociation. Also, the percentage of bonds with a slow off-rate increased significantly, from 20% to 74%, at the expense of the fast

dissociation population of bonds, which decreased from 80% to 26%. A ten second cut off had to be used to since longer lifetime measurements would be susceptible to significant amounts of drift.

The manganese condition produced two distinct off-rate populations which can also be seen in the two distinct slopes made by the blue data points in figure 4-3. And, just as in the magnesium/EGTA case, the slope of both distributions decreased significantly when primed, implying longer lived bonds. The percentage of bonds with a slow off-rate increased from 12% to 40% while the fast dissociation population decreased from 88% to 60%.

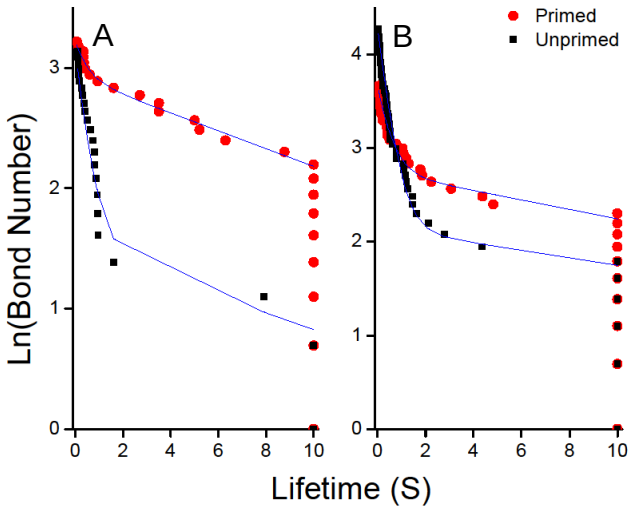

Figure 4-3. Natural log plot of the $\alpha_5\beta_1$ lifetimes. A) A plot of the natural log of the bond number for the magnesium/EGTA experiments. B) A plot of the natural log of the bond number for the manganese experiments. Both the primed and unprimed data is shown along with the curve fit (blue line) used to approximate the off-rates and off-rate fractions.

When looking at the data presented in figure 4-3, two possibilities exist for the data points that last till the ten second cutoff. The first is that at least some of these points belong to a third off-rate distribution that could not be seen on this time scale. The other is that these bonds belong to the off-rate distribution that

makes up the gently sloped regions that can be observed here. Since we have no data to prove the existence of an even longer lived region, the lifetimes that lasted longer than ten seconds will be counted together with the lifetimes that do not make up the highest off-rate distribution.

The results shown for both metal ion conditions draw a strong parallel with the purified molecule results. In both cases the binding without priming is very weak, with a very high percentage of fast off-rate dissociations, but improves drastically with priming (figure 4-4). Also, interestingly the magnesium/EGTA case had stronger binding than the manganese case in the $\alpha_5\beta_1$-FC chimera work as well as here (figure 4-4). Clearly this was surprising, both in this work and the previous work, given the commonly held belief that manganese, though not physiologically relevant, induces stronger binding.

In both metal ion conditions, most of the lifetimes for the nonprime state fall below two seconds while a noticeable shift toward slower off-rates can be seen in the primed conditions (figure 4-3). The magnesium/EGTA condition when primed had a fairly even spread across the span of lifetimes. In contrast, the primed magnesium condition has a large gap in both the primed and unprimed conditions between six and ten seconds. This observation leads to another. Only a handful of lifetimes in the manganese primed condition that lasted longer than the initial region dominated by the fast off-rate term do not make the ten second cutoff.

Surprisingly, the similarities in the data presented for this work are even more apparent when the off-rate fractions of the primed and unprimed groups are

compared (figure 4-4). It has been observed that the metal ion condition greatly affects the affinity of the receptor (43, 49). While this is not borne out for the unprimed case on live cells, it should be understood from this data that the metal ion condition did have a noticeable effect on the percentage of fast off-rate events observed when the bond was primed (figure 4-4). Viewing this in light of the effect metal ion condition has on the global conformation distribution, it can be interpreted that in the unprimed case metal ion condition does not greatly affect the percentages of off-rates seen. However, when primed, the off-rate does depend on the metal ion condition of the receptor.

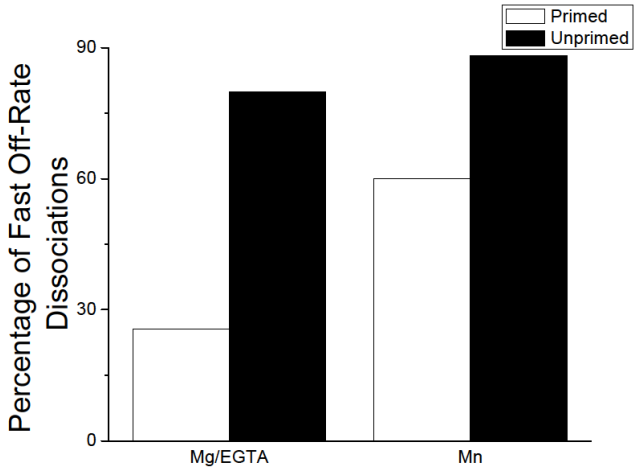

Figure 4-4. Fast off-rate percentages of $\alpha_5\beta_1$ force priming experiment. An illustration of the effects of force priming on the percentages of fast off-rate dissociations.

Finally, the two off-rate parameters, slow and fast, found from the fit have units of inverse second. Therefore taking the inverse of the off-rates found gives a characteristic time for each distribution with the larger numbers obviously correlating with longer lived groups of bonds. When the inverse off-rates taken from the fit are compared, the effect of force priming on the exhibited off-rates is surprising (figure 4-5 and figure 4-6). In figure 4-5, the inverse of the fast off-rates

have very similar values. The same can be said, though not as strongly, about the inverse of the slow off-rates illustrated in figure 4-6. While there is a small change in the manganese case, looking at the entirety of figure 4-5 and figure 4-6, it is obvious that force priming does not significantly change the observed off-rates.

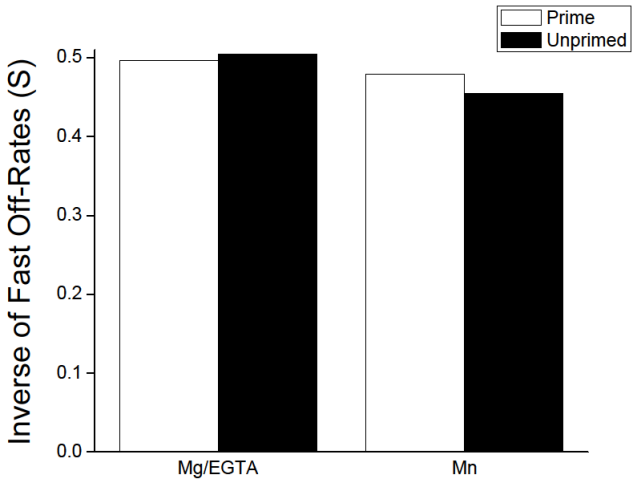

Figure 4-5. Inverse fast off-rate of primed and unprimed events. The inverse of the off-rates for the primed and unprimed off-rate distribution seen under the magnesium/EGTA and manganese conditions.

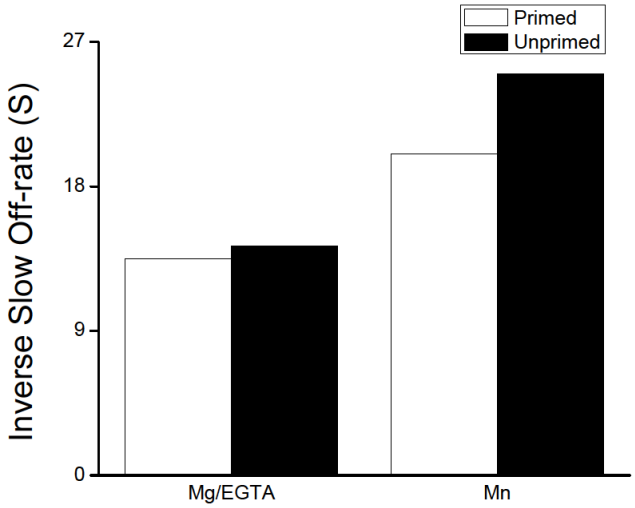

Figure 4-6. Inverse slow off-rates of primed and unprimed events. The inverse of the off-rates for the primed and unprimed off-rate distribution seen under the magnesium/EGTA and manganese conditions.

Looking this data as a whole, $\alpha_5\beta_1$ has a higher percentage of lifetimes that last till the ten second lifetime when primed. Also, priming causes a higher percentage of slow off-rate dissociations but does not change the off-rates observed. The longer binding that was seen in the primed case then was not because of the intrinsic kinetics of the bond changing, but an increase in the propensity of the primed bond to exist in its already occurring slower dissociation state.

Force-Priming Effect on I Domain Possessing Integrin

Next we sought to understand the effects of force priming on integrin possessing an I domain. As stated previously, the I domain replaces the I-like domain and β propeller as the ligand binding site. Therefore, from this experiment a significant amount of insight can be made into the relationship between integrin's structure and the force priming phenomenon.

Previously, work had been done on force regulation of LFA-1 binding [28]. This work, done on similar cells and using a similar machine and technique, however using human ICAM-1 instead of mouse ICAM-1, established that LFA-1 does indeed exhibit a catch bond which is strongest at ~15pN for a variety of conditions and cases (figure 2-12). Therefore the priming case was investigated by priming the bond to ~15pN before relaxing the bond to ~5pN.

Before the other experiments were done, a series of controls were performed to demonstrate specific binding between LFA-1 and its the ligand. The adhesion frequency of a Jurkat cell and a bead coated with streptavidin but no ligand was measured to quantify the amount of nonspecific interactions. As

expected, the adhesion frequency of this test fell below the adhesion frequency measured when the actual experiment was run (figure 4-7).

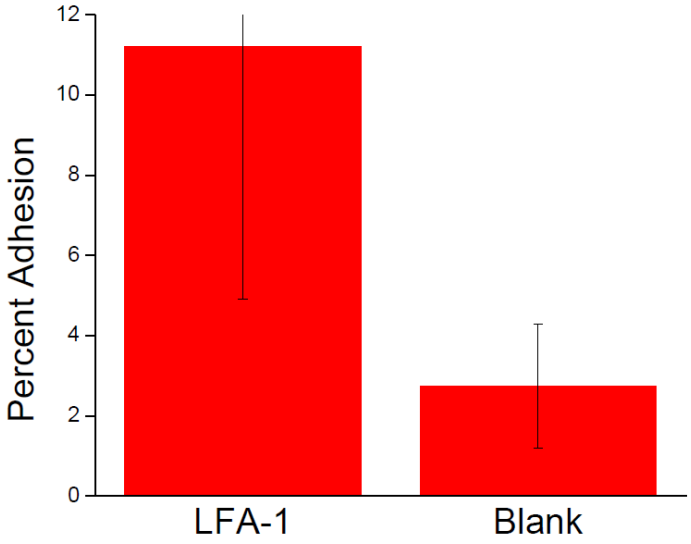

Figure 4-7. Adhesion frequency versus blank control.

In this case, we also hypothesized that a priming event would greatly increase the lifetime of the bond since a catch bond had previously been observed [28]. However, the absence of a synergy site did not lend itself toward our hypothesis [45]. If there was no noticeable effect due to priming, then it is very likely that the synergy site plays a strong role. However, this was not the case.

The dissociation rate between the two states also changed a great deal as expected (figure 4-8). The natural log plot of the lifetimes measured again can be fit using the two off-rate model that was used in the $\alpha_5\beta_1$ experiments, with two off-rates, for both the force primed and unprimed data sets. Here the increased bond lifetime is due to a change in the intrinsic kinetics. The difference between

the primed and unprimed case is immediately apparent in the overall shape of the fit in each case.

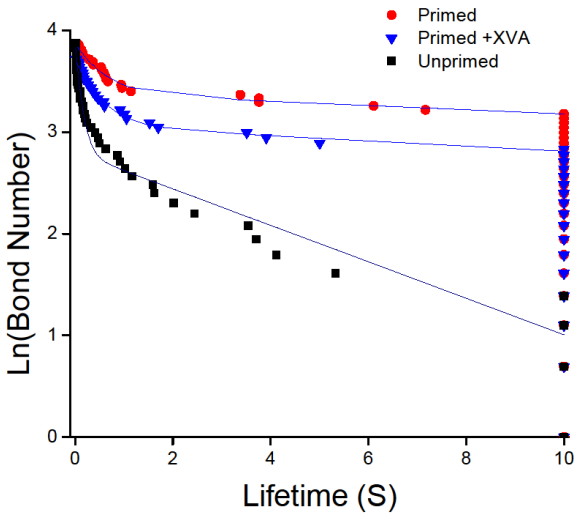

Figure 4-8. Natural log plot of LFA-1 experiment. A plot of the natural log of the bond number for the LFA-1 experiments. The primed, primed in the presence of XVA-143 and unprimed data is shown along with the curve fit (blue line) used to approximate the off-rates and off-rate fractions.

Likewise, the percentage of lifetimes that exceeded the ten second cut off increased not only over the nonprimed case but also over the $\alpha_5\beta_1$ case, from 8.3% to 50% (figure 4-9). Also, LFA-1 saw a similar decrease in the percentage of fast off-rate dissociations when the bond was primed, falling from 66% to 35% (figure 4-10). Conversely, the application of the priming force increased the percentage of slow off-rate binding events from 34% to 65%. Most likely, while the synergy site might play a role, it is not required for this type of phenomenon.

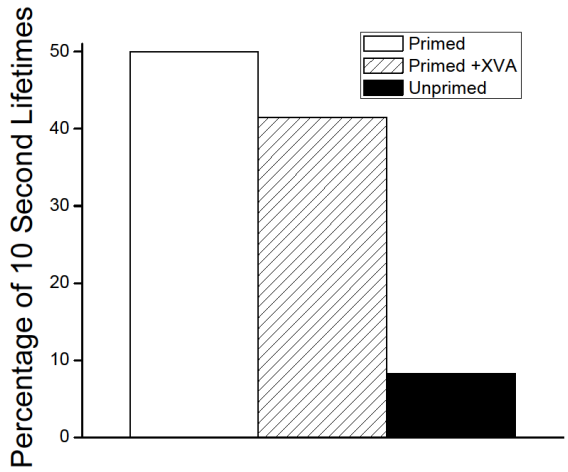

Figure 4-9. Percentage of LFA-1 ten second lifetimes.

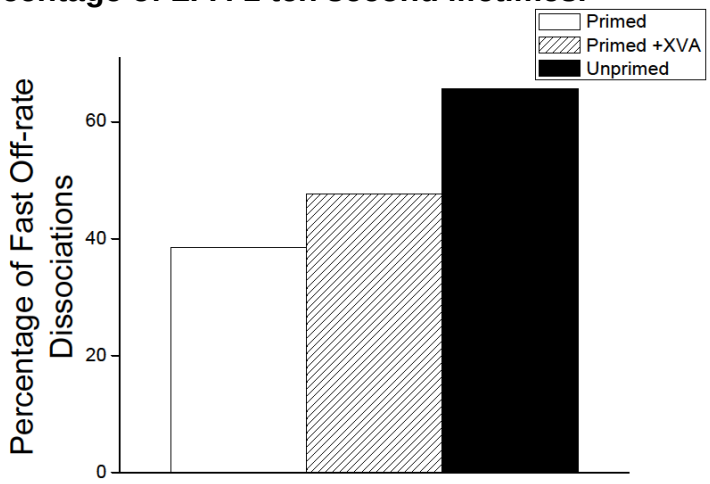

Figure 4-10. Percentage of LFA-1 fast off-rate dissociation. For each of the three experiments run on LFA-1, the natural log of the bond number versus the lifetime was fit with a two off-rate model. The percentage of the slow off-rate dissociations is shown here.

Effect of XVA-143 on the Force Priming Phenomenon

XVA-143, a small molecule allosteric inhibitor, was used here to further understand the conformational effects of the LFA-1 binding pocket on force priming. Normally XVA-143 is associated with weaker binding by I domain containing integrin. As can be seen in the data, while this is true, the effect was not significant if the bond lasted through the priming force (figure 4-9 and figure 4-10). When the total number of adhesion, including bonds that ruptured during

the priming event were taken into accounted the effects XVA-143 has an on binding and adhesion are obvious (figure 4-11). These values were found by multiplying the total number of lifetimes measured by the off-rate fractions found from fitting the dual off-rate model to the data to get the actual number of fast and slow off-rate dissociation events. Then the number of bond ruptures that did not last past the priming event were added to the fast off-rate dissociation events to get the total number of weak bonds. Finally, both the number of slow off-rate dissociation events and the weak bonds and were divided by the sum of the number of lifetimes and rupture events to get a percentage for each.

However, if only bonds that survived the priming event are counted, then it can be seen that XVA-143 does not significantly affect force priming (figure 4-12 and figure 4-13). Under the primed XVA-143 condition the percent of lifetimes that reached ten seconds was 43.9%, only 6.1%; less than the non-inhibited case. This was very unexpected given data previously taken concerning XVA-143's effect on the LFA-1 catch bond. In his thesis, Chen shows that the presence of XVA-143 abolishes the catch bond mentioned previously [28]. It is worth mentioning again, however, that this data was taken using a different ligand.

The force activated data presented here shows two off-rate distributions very much like the $\alpha_5\beta_1$ manganese case, all the LFA-1 experiments show a two slope distribution (figure 4-8). However, as can be seen when the two off-rates from the fit are compared (fig 4-8), the off-rates change in a dramatic manner between either the primed condition and the unprimed condition but is not

affected by the presence of XVA-143. This change in off-rates is the marked difference between the two experiments. But most importantly, a significant number of bonds in the presence or absence of XVA-143 persisted until the ten second cutoff, very much like the $\alpha_5\beta_1$ data shown earlier.

As before, the off-rates found from the fit of the LFA-1 data have a unit of inverse second. Therefore, taking the inverse of each gives a characteristic time for each distribution with the larger numbers obviously correlating with longer lived groups of bonds. As can be seen in figure 4-12 and 4-13, the LFA-1 off-rates for either primed condition, while varying slightly, does demonstrate a massive change. When either of these are compared to the unprimed case though a significant change is seen as opposed to the $\alpha_5\beta_1$ case.

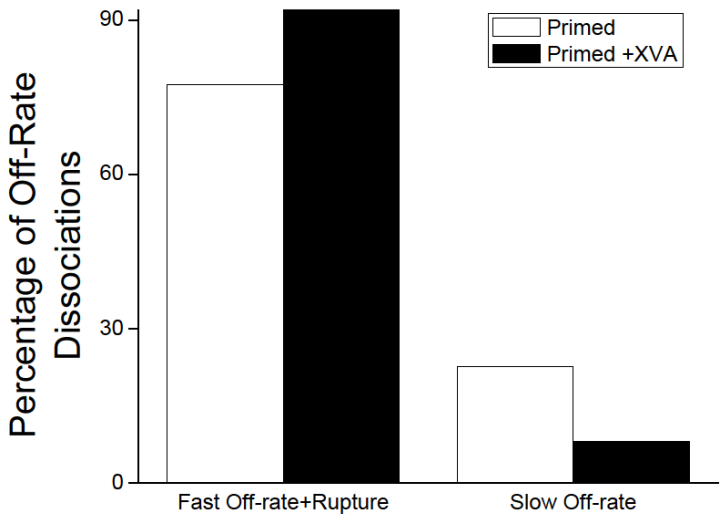

Figure 4-11. Effects of XVA-143. When rupture events were counted with the fast off-rate, short lifetime events, the effect of XVA-143 became noticeable.

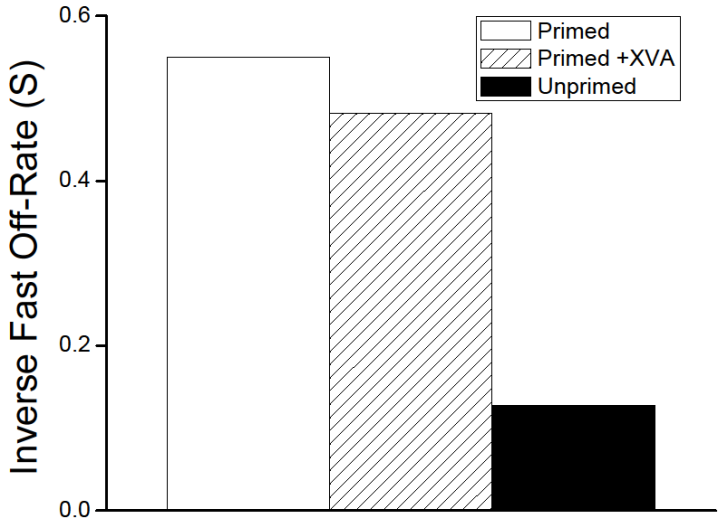

Figure 4-12. Inverse of the LFA-1 fast off-rates.

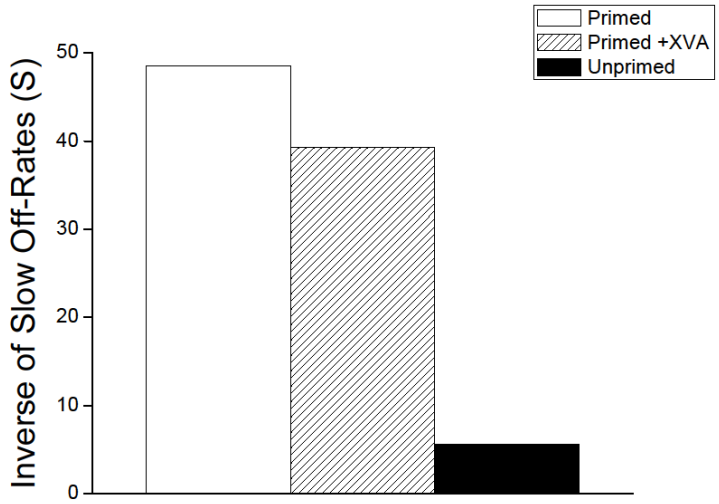

Figure 4-13. Inverse of the LFA-1 slow off-rates.

CHAPTER 5

DISCUSSION

When considering both types of integrin and the number of conditions used, it becomes extremely evident that a phenomenon such as force priming can strengthen binding on live cells. This phenomenon had previously been shown to exist with purified integrin-FC chimera [27]. This study extends that to show that this event type is still present with whole integrin possessing both the transmembrane portion and intracellular tails supported in a cell membrane while being controlled by a living cell. Typically the transmembrane and tail portions are thought to inhibit strong binding since the presence of these allows the legs to associate and bend [15, 55]. Likewise, this study demonstrates that there are no adaptor proteins or other cellular controls present in living cells that abolish force priming. Also, it is logical to assume that this is a useful observation for understanding the catch bond behavior previously seen in integrins [27,28].

A similar observation was previously reported using $\alpha_5\beta_1$ expressing HT1080 cells by first allowing the cells to adhere to the surface of a disk coated in the same fibronectin fragment used in this study [45]. Then, the bonds were tensioned when the disk was spun. Finally the number of bonds was measured by ratios of arbitrary units of Western blot intensity. The authors of this study observed that the tensioning did not cause an increase in bond number. Instead they observed that, after the application of the shear force, the number of bonds decreased. However, the bonds that remained were more easily chemically cross-linked implying a more substantial contact area between the ligand and

receptor. The authors then go on to attribute the observed increase in bond strength to the engagement of the synergy site in the β propeller of the α subunit to the fibronectin fragment. In effect, the authors of this paper are implying force activation in their work since the cross linking took place under no force after the application of shear. While the author's conclusions are reasonable, in light of the results shown here, this is an incomplete explanation. Using their conclusions, it is unlikely that a force priming event would be seen in an integrin possessing an I domain. The reason for this is that an I domain possessing integrin has only one binding site while an I domain lacking integrin, such as $\alpha_5\beta_1$, binds its ligand at two locations [44, 45]. Since there is no opportunity for multiple engagements between a single receptor/ligand pair with I domain possessing integrin, there must be either a decrease in the off-rate associated with the priming force or a change in the likelihood of the preexisting off-rates. In effect, instead of simply stating that stronger integrin bond strength seen in the paper [45] is caused by multiple binding, the data presented here implies that, at least in the I domain containing case, the off-rate can indeed change disassociation constants. More importantly, this data also demonstrates that a large initial force can change the percentage of slow versus fast off-rate events without the need to maintain the force for the lifetime of the bond. This then seems to be the most likely, indeed the simplest, explanation so far for force priming for all integrins.

Furthermore, the data presented in this work demonstrates that the $\alpha_5\beta_1$ off-rates seen under all of the conditions did not change drastically with priming. If the bonds that survived have similar off-rates to bonds formed without a

priming event then the binding pockets after priming likely have similar conformations. However the propensity for slowest off-rates and longer lived bonds increased dramatically when the bond is primed. Also, given the data taken in the presence of both metal ion conditions, it is clear that there is a definite correlation between the change in off-rates seen and the global conformation. In figure 4-2 and 4-4, the manganese data showed lower percentage of bonds that lasted to the ten second threshold and a higher percentage of fast off-rate dissociations than the magnesium/EGTA condition. As said before in the introduction, manganese exhibits a mostly extended population while magnesium/EGTA is believed to have a more bent population. Given its inherent flexibility, it is possible that the priming force could cause bent integrin to extend. It is then reasonable to hypothesize that this extension could cause the observed differences

The other, major case studied here was priming in the presence of XVA-143. The similarities in the off-rates and off-rate fractions demonstrated here shows that, while one position might be favorable for force activation, there is no one specific head piece conformation that is required for successful priming. It is possible that priming can cause the necessary movement of the α1 helix through a different pathway that does not require the α7 helix to shift down. XVA-143 is known to effect binding by disrupting the interface between the I-like and I domain. If priming can cause a conformational change in the I domain then it could increase the binding strength without necessitating any interplay between the I domain and the lower headpiece.

In light of the data gathered under different metal ion conditions and in the presence versus absence of an allosteric inhibitor, it appears that the dramatic effects of priming are both local and global in nature. This is in partial opposition to the finding of the purified $\alpha_5\beta_1$ experiment. In that study, the catch bond and force activation data for $\alpha_5\beta_1$, evaluated under several metal ion conditions, implied that both the increase in the binding strength are seen in a similar manner in the binding pocket without regardless of the conformation of the rest of the dimer which therefore implies a local conformation change in the binding pocket. No such conclusion can be made here.

What is surprising is the relation between this work and the previous work done to confirm the existence of the $\alpha_5\beta_1$ catch bond. The same ligand was used both in this work and in the one that established the catch bond [27]. Therefore the force that was exerted on the binding pocket was exerted in a similar direction and to the same I-like domain residues and secondary structures. In this work the bonds lasted longer but only by transitioning to dissociation rates that previously existed with a lower probability of being observed. By its strictest definition, this is not catch bond behavior. What seems most likely here is that the I-like domain requires the force to be exerted throughout the bond to maintain the new off-rates. If force priming event takes place and then the force is relaxed the α1 helix in the I-like domain might attempt to return to one of the positions it naturally takes under a lower force. If the position associated with longer lived bonds is energetically the closest position to return to then a longer lifetime is

observed. If this is the case then the priming event biases the α1 helix position in the I -like domain toward the longer lived events.

The next question then is what is the difference between the I domain lacking and containing cases. When comparing the binding pocket between the I domain and I-like domain, one feature that stands out is the ADMIDAS site in the I-like domain. The ADMIDAS site has previously been shown not to be directly involved in ligand binding [46]. Instead it has an allosteric regulatory effect on the other metal ion sites involved in binding, namely the MIDAS site. The ADMIDAS site might be able to regulate the I-like domain's binding pocket during the bond, by requiring a high sustained force to maintain a change in the intrinsic off-rates. Meanwhile, the I-domain, lacking an ADMIDAS site, would not require the force to be exerted for the duration of the bond lifetime to notice a similar effect.

No one has been able to conclusively explain the purpose of the I domain. Perhaps this then is the purpose of the I domain; to act as a switch that can shift the integrin to lower off-rates when the bond experiences a strong, transient force. When looking at the range of integrin structures, the I domain at first seems unnecessary. However, if I domain lacking integrin regulate their binding according to changes in the force experienced while the receptor is bound then it is easy to see why the I domain might be necessary in some cases.

CHAPTER 6

CONCLUSION

Understanding integrin binding is a difficult problem. This thesis explored one interesting characteristic of it but this needs to be explored more fully. This thesis served to elucidate some aspects, namely that any force related integrin activation is effected strongly by the global conformation of the receptor. However, if the activation can take place regardless of the initial conformation, which is likely since both metal ion conditions were able to be activated by force then it is not purely the extension of the receptor that is required either. Further work needs to be done on the activation requirements of the I and I-like domains. LFA-1 showed behavior similar to that seen in catch bonds when activated by force. Conversely, $\alpha_5\beta_1$ did not. Instead $\alpha_5\beta_1$simply shifted between preexisting off-rates when activated by force. XVA-143, a molecule believed to allosterically inhibit I domain containing integrin such as LFA-1, proved ineffective at abolishing the force priming effects seen here but have been shown to transition the catch bond seen in LFA-1 to a slip bond. This is both unexpected and very interesting.

CHAPTER 7

FUTURE RECOMMENDATIONS

After completing this work, it has become apparent to the author that integrin is certainly a complex and interesting research area. More work must be done as we are only beginning to understand the complexities involved. With an eye toward advancing that understanding, the author believes the following steps should be taken.

Firstly, integrin research, and all receptor research actually, is based primarily on the physics of binding, the structure of the molecules involved and the intracellular and intercellular signaling that is involved. The physics of binding is of course an important place to start. It is the function being studied in most cases. Signaling events, whether inter- or intracellular, are the other function. And finally the structure of the molecules provides scientists with the opportunities to put the physics of binding to use with our understanding of signaling events to help patients. This field does exist after all, for the eventual care of patients.

If the hypothesis presented here, that the I domain is responsible for the different responses seen in $\alpha_5\beta_1$ and LFA-1 to force activation, is to be tested then the I domain and I-like domain on live cell integrin should be somehow altered, most suitably by a transfecting an I or I-like domain possessing integrin with either α1 helix locked in a fixed position into a live cell. These cells could then be used to repeat the force activation experiments or in a flow chamber experiment where the shear force is varied in a fashion similar to what was used

here. Finally, the most direct way to understand this question would be a molecule dynamics situation where the force is exerted through the ligand binding site and then relaxed while paying close attention to the α1 helix position compared to a constant force simulation. Another interesting set of simulations would be using the headpiece of an integrin lacking an I domain loaded in a similar fashion. A comparison between the two could shed a significant amount of light on both the phenomenon of force activation as well possibly the purpose of the I domain.

The other imperative to continue this work is the intercellular signaling events. Integrin is a well known and important signaling receptor. It is also hypothesized by many to be the key to the question, “mechanically, how do cells sense their environment?”. If we are to answer this question then we must determine if and how single molecule pair binding is affected by the force of the bond. Does the force of the bond affect the signaling of the integrin into the cell? Does the force history of the bond affect the signaling into the cell? Does force activation increase or change the signaling events mediated by the integrin inside the membrane? What is the prerequisite force to incite signaling? These questions are just the tip of a much larger iceberg concerning the force-signaling relationship. To answer these, the BFP system must integrate fluorescent imaging. Integrating the ability to read fluorescence during an experiment opens up the possibility of using intracellular fluorescent sensors to examine how force affects signaling. If this is done properly then these experiments might yet

answer whether integrin can actually sense and communicate the mechanical environment the cell is exposed to.

Finally, the BFP, while an incredibly useful technique for characterizing binding must improve to make further progress. Currently the BFP can drift significantly over large time periods. While this was not quantified and depends on the quality of the bead placement, a drift of 2 pN in ten seconds would not be uncharacteristic. Indeed in a BFP experiment a number of lifetimes have to be discarded because the measured force drifts a unacceptable amount. To measure longer binding events a scheme to compensate for this must be implemented. Currently there are three drifting components that can affect the measurement of long lived bonds in BFP experiments: drifting of the objective lens, drifting of the probe pipette which holds the RBC-bead pair and drifting of the target pipette holding the cell expressing the receptor being studied. Currently commercially available systems to compensate for drift of the objective lens are available. The other two will require a more innovative solution, most likely involving mounting these pipettes on piezo electric manipulators that can be controlled by a computer to compensate their position. If all three of these are controlled then the BFP opens itself up to investigating much low off rate binding. Indeed theoretically these could allow a near infinity bond lifetime limit.

REFERENCES

1. Shimaoka M, Salas A, Yang W, Weitz-Schmidt G, Springer T.A. (2003) Small olecule integrin antagonists that bind to the beta 2 subunit I-like domain and activate signals in one direction and block them in the other. *Immunity* 19:391-402

2. Luo BH, Carman CV, Springer TA (2007) Structural basis of integrin regulation and signaling. *Annu Rev Immunol* 25:619-647

3. Michishita M, Videm V, Arnaout MA (1993) A novel divalent cation-binding site in the A domain of the beta 2 integrin CR3 (CD11b/CD18) is essential for ligand binding. *Cell* 72:857–67

4. Hynes RO (2002) Integrins: bidirectional, allosteric signaling machines. *Cell* 110:673-687

5. Xiong JP, Stehle T, Diefenbach B, Zhang R, Dunker R*, et al.* (2001) Crystal structure of the extracellular segment of integrin aVb3. *Science* 294:339-345

6. Xiong J-P, Stehle T, Zhang R, Joachinliak A, Frech M*, et al.* (2002) Crystal Structure of the Extracellular Segment of Integrin a_Vb_3 in Complex with an Arg-Gly-Asp Ligand. *Science* 296:151

7. Carrell NA, Fitzgerald LA, Steiner B, Erickson HP, Phillips DR (1985) Structure of human platelet membrane glycoproteins IIb and IIIa as determined by electron microscopy. *J. Biol. Chem.* 260:1743-1749

8. Weisel J, Nagaswami C, Vilaire G, Bennett J (1992) Examination of the platelet membrane glycoprotein IIb-IIIa complex and its interaction with fibrinogen and other ligands by electron microscopy. *J. Biol. Chem.* 267:16637-16643

9. Wippler J, Kouns W, Schlaeger E, Kuhn H, Hadvary P*, et al.* (1994) The integrin alpha IIb-beta 3, platelet glycoprotein IIb-IIIa, can form a functionally active heterodimer complex without the cysteine-rich repeats of the beta 3 subunit. *J. Biol. Chem.* 269:8754-8761

10. Takagi J, Petre BM, Walz T, Springer TA (2002) Global conformational rearrangements in Integrin extracellular domains in outside-In and inside-out signaling. *Cell* 110:599-611

11. Parise L, Helgerson S, Steiner B, Nannizzi L, Phillips D (1987) Synthetic peptides derived from fibrinogen and fibronectin change the conformation of purified platelet glycoprotein IIb-IIIa. *J. Biol. Chem.* 262:12597-12602

12. Beglova N, Blacklow SC, Takagi J, Springer TA (2002) Cysteine-rich module structure reveals a fulcrum for integrin rearrangement upon activation. *Nature Structural Biology* 9:282

13. Shimaoka M, T.A. Springer (2003) Theurapeutic antagonists and conformational regulation of integrin function. *Nat Rev Drug Discov* 2:703-716

14. Lau T.L., Kim C, Ginsberg M, Ulmer T (2009) The structure of the integrin αIIbβ3 transmembrane complex explains integrin transmembrane signaling. *The EMBO Journal* 28:1351-1361

15. Xiao T, Takagi J, Coller BS, Wang JH, Springer TA (2004) Structural basis for allostery in integrins and binding to fibrinogen-mimetic therapeutics. *Nature* 432:59-675

16. Xiong J.P., Stehle T, Goodman S.L., M.A. Arnaout (2003) New insight into the structural basis of integrin activation. *Blood* 102:1155-1159

17. Harding MM. 2001. Geometry of metal-ligand interactions in proteins. *Acta Crystallogr. D* 57:401–11

18. Karpusas M, Ferrant J, Weinreb P.H., Carmillo A, Taylor F.R., Garber E.A. (2003) Crystal structure of the alpha1beta1 integrin I domain in complex with an antibody Fab fragment. *Journal of Molecular Biology* 327:1031–41

19. Shimaoka M, Xiao T, Liu J.H., Yang Y, Dong Y, Jun C.D., McCormack A, Zhang A, Joachimiak A, Takagi J, Wang J.H., Springer T.A. (2003) Structure of the alpha L I domainand its comples with ICAM-1 reveal a shape-shifting pathway for integrin regulation. *Cell* 112:99-111

20. Lu C, Shimaoka M, Zang Q, Takagi J, Springer T.A. (2001) Locking in alternative conformations of the integrin alphaLbeta2 I domain with disulfide bonds reveals functional relationships among integrin domains. *Proceedings of the National Academy of Science*, 98:2393-2398

21. Carman C, Springer T.A. (2003) Integrin avidity regulation: are changes in affinity and conformation underemphasized?. *Current Opinion in Cellular Biology* 15:547-556

22. Puklin-Faucher E, Sheetz M (2009) The mechanical integrin cycle. *Journal of cell Science* 122:179-186

23. Woolf E, Grigorova I, Sagiv A, Grabovsky V, Feigelson S, Shulman Z, Hartmann T, Sixt M, Cyster J, Alon R (2007) Lymph node chemokines promote sustained T lymphocyte motility without triggering stable integrin adhesiveness in the absence of shear forces. *Nature Immunology* 8:1076-1085

24. Giancotti F, Ruoslahti E (1999) Integrin Signaling. *Science* 285: 1028

25. Astrof NS, Salas A, Shimaoka M, Chen J, Springer TA (2006) Importance of force linkage in mechanochemistry of adhesion receptors. *Biochemistry* 45:15020-15028

26. Balaban NQ, Schwarz US, Riveline D, Goichberg P, Tzur G*, et al.* (2001) Force and focal adhesion assembly: a close relationship studied using elastic micropatterned substrates. *Nat Cell Biol* 3:466-472

27. Fang K, Integrin $\alpha_5\beta_1$ and fibronectin interaction under force (2008) Mechanical Engineering Department, Georgia Institute of Technology: Atlanta

28. Chen W, Force regulation on binding kinetics and conformations of integrin and selectins using a bio-membrane force probe, (2009) Mechanical Engineering Department, Georgia Institute of Technology: Atlanta

29. Zhang F, The regulation of conformation and binding kinetics of alphaLbeta2 (2007) Biomedical Department, Georgia Institute of Technology: Atlanta

30. Merkel R, Nassoy P, Leung A, Ritchie K, Evans E (2001) Probing the relation between force-lifetime and chemistry in single molecular bonds. *Ann. Rev. Biophys. Biomol. Struct.* 30:105-128

31. Merkel R, Nassoy P , Leung A, Ritchie K, Evans E (1999) Energy landscapes of receptor-ligand bonds explored with dynamic force specroscopy. *Nature* 397:50-53

32. Marshall BT, Long M, Piper JW, Yago T, McEver RP*, et al.* (2003) Direct observation of catch bonds involving cell-adhesion molecules. *Nature* 423:190-193

33. Bell GI (1978) Models for the specific adhesion of cells to cells. *Science* 200:618-627

34. Evans E, Ritchie K (1997) Dynamic strength of molecular adhesion bonds. *Biophysical Journal* 72:1541-1555

35. Dembo M, Tourney D.C., Saxman K, Hammer D (1988) The reaction-limited kinetics of membrane-to-surface adhesion and detachment. *Pro. R. Soc. Lond. B.* 203:55-83

36. Yago T, Lou J, Wu T, Yang J, Miner J.J., Coburn L, Lopez J.A., Cruz M.A., Dong JF, McIntire L.V., McEver R.P., Zhu C (2008) Platelet glycoprotein Ibα forms catch bonds with WT vWF but not type 2b von Willebrand disease vWF. *Journal of Clinical Investigations* 118:3195-3207

37. Yakovenko O, Sharma S, Forero M, Tchesnokova V, Aprikian P, Kidd B, Mach A, Vogel V, Sokurenko E, Thomas W.E. (2008) FimH forms catch bonds that are enhanced by mechanical force due to allosteric regulation. *Journal of Biological Chemistry* 283:11596-11605

38. Binning G, Quate C, Gerber C (1986) Atomic force microscope. *Phys. Rev. Lett*. 56:930-933

39. Ashkin A (1997) Optical trapping and manipulation of neutral particles using lasers. *Proceedings of the National Academy of Science* 94:4853-4860

40. Ashkin A (1992) Force of a single-beam gradient laser trap on a dielectric sphere in the ray optics regime. *Biophysical Journal* 61:569

41. Evans E (1999) Looking inside molecular bonds at biological interfaces with dynamic force spectroscopy. *Biophysical Chemistry* 82:83-97

42. Evans E, Ritchie K, Merkel R (1995) Sensitive force technique to probe molecular adhesion and structural linkage at biological interface. *Biophysical Journal* 68:2580-2587

43. Chen L.L., Whitty A, Scott D, Lee W.C., Adams S.P., Petter R.C., Lobb R.R., Pepinsky R.B. (2001) Evidence that ligand and metal ion binding to integrin alpha4 beta1 are regulated through a coupled equilibrium. *Journal of Biological Chemistry* 276:36520-36529

44. Takagi J, Takagi K, Springer T.A. (2003) Structure of integrin $\alpha_5\beta_1$ in complex with fibronectin. EMBO Journal 22:4607-4615

45. Friedland J, Lee M, Boettiger D (2009) Mechanically activated integrin switch controls $\alpha_5\beta_1$ function. *Science* 323:642-644

46. Mould A, Barton S, Askari J, Craig S, Humphries (2003) Role of ADMIDAS cation-binding site in ligand recognition by integrin $\alpha_5\beta_1$, *The Journal of Biological Chemistry* 51:51622-51629

47. Leahy D, Aukhil I, Erickson H (1996) 2.0 A crystal structure of a four-domain segment of human fibronectin encompassing the RGD loop and the synergy region. *Cell* 84:155-164

48. Anderson D, Springer T.A. (1987) Leukocyte Adhesion deficiency: an inherited defect in Mac-1, LFA-1, and p150,95 glycoporteins. *Annual Review of Medicine* 38:175-194

49. Chen J, Salas A, Springer T.A. (2003) Bistable regulation of integrin adhesiveness by a bipolar metal ion cluster. *Nature Structural Biology* 10:995-1001

50. Roca-Cusachs P, Gauthier N, del Rio A, Sheetz M (2009) Clustering of $\alpha_5\beta_1$ integrins determines adhesion strength whereas $\alpha_V\beta_3$ and talin enable mechanotransduction. *Proceedings of the National Academy of Science USA* 106:16245-16250

51. Guo B, Guilford W (2006) Mechanics of actomyosin bonds in different nucleotidestates are tuned to muscle contraction. *Proceedings of the National Academy of Science USA* 103:9844–49

52. Huang C, Springer TA (1995) A binding interface on the I domain of lymphocyte function-associated antigen (LFA-1) required for specific interaction with intercellular adhesion molecule 1 (ICAM-1). *Biophysical Journal* 270:19008-19016

53. Katagiri K, Hattori M, Minato N, Irie S, Takatsu K, Kinashi T (2000) Rap1 is a potent activation signal leukocyte function-associated antigen 1 distinct from protein kinase c and phosphatidylinositol-3-OH kinase. *Molecular and Cellular Biology* 20:1956-1969

54. Zhu C, Long M, Chealsea SE, Bongrand P (2002) Measuring receptor/Ligand interactions at the single bond level:experimental and interpretative issues. *Annals of Biomedical Engineering* 30:305-314

55. Wegender KL, Patridge AW, Ginsberg MH (2005) Integrin activation by talin. *Journal of Thrombosis and Haemostasis: JTH* 3:1783-1790

56. Sarangapani K et. al. (2004) Low force decelerates L-Selectin dissociation from P-selectin glycoprotein ligand-1 and endoglycan. *Journal of Biological Chemistry* 279: 2291-2298

57. Hemler M et. al. (1987) Characterization of the cell surface heterodimer VLA-4 and related peptides. *The Journal of Biological Chemistry* 262: 11478-11485